IMMUNOLOGY

Perfect adaptation of CD8$^+$ T cell responses to constant antigen input over a wide range of affinities is overcome by costimulation

Nicola Trendel[1]*†, Philipp Kruger[1]*‡, Stephanie Gaglione[1]*§, John Nguyen[1], Johannes Pettmann[1,2], Eduardo D. Sontag[3], Omer Dushek[1]||

Maintaining and limiting T cell responses to constant stimulation with antigen are critical to control pathogens and maintain self-tolerance, respectively. Antigen recognition by T cell receptors (TCRs) activates signaling that stimulates T cells to produce cytokines and also leads to the down-regulation of cell surface TCRs. In other systems, receptor down-regulation can induce perfect adaptation to constant stimulation by a mechanism known as state-dependent inactivation, which requires complete down-regulation of the receptor or the ligand; however, this is not the case for the TCR. Here, we observed that in vitro–expanded primary human T cells exhibited perfect adaptation with respect to cytokine production to constant antigen stimulation across a 100,000-fold variation in affinity with partial TCR down-regulation. By directly fitting a mechanistic model to these data, we showed that TCR down-regulation produced imperfect adaptation, but, when coupled to a switch, produced perfect adaptation in terms of cytokine production. A prediction of this model was that TCR signaling induced by peptide-bound major histocompatibility complex (pMHC) continues after adaptation, which we confirmed by showing that, whereas costimulation could not prevent adaptation, signaling by the costimulatory receptors CD28 and 4-1BB reactivated adapted T cells to produce cytokines in a pMHC-dependent manner. We showed that adaptation also applied to first-generation chimeric antigen receptor (CAR) T cells but was partially avoided with second-generation CARs. These findings highlight that perfect adaptation limits the responses of T cells, rendering them dependent on costimulation for sustained responses.

INTRODUCTION

T cell activation, which is critical to initiate and maintain adaptive immunity, proceeds by the recognition of antigens in the form of peptide-bound major histocompatibility complexes (pMHCs) by T cells through their T cell receptors (TCRs). TCR/pMHC binding induces signaling pathways that stimulate T cells to directly kill cancerous or infected cells and to secrete a range of cytokines (*1*). When T cells are confronted with persistent or constant pMHC antigens, maintaining responses to foreign or altered-self pMHC [in chronic infections and cancers (*2*)] can be just as important as limiting responses to self pMHC [for example, adaptive tolerance (*3*)]. Similarly to other surface receptors, the TCR is down-regulated from the surface of T cells upon recognition of pMHC ligands (*4*). Precisely how TCR down-regulation controls T cell responses to constant pMHC stimulation remains controversial.

In other cellular systems, receptor down-regulation can induce biological adaptation to constant ligand stimulation (*5*). Adaptation is defined by the ability of a system to display transient responses that return to baseline when presented with constant input stimulation. The process is known as perfect (or near-perfect) when the baselines before and after stimulation are similar; otherwise, it is imperfect. Systematic network searches have identified two key mechanisms of adaptation: negative feedback loops and incoherent feedforward loops (IFFLs) (*6*, *7*). At a molecular level, these mechanisms are implemented by cell surface receptors, signaling pathways, and transcriptional networks (*5*, *8*, *9*). In the case of receptor tyrosine kinases, G protein–coupled receptors, and ion channels, the common underlying mechanism is effectively an IFFL termed as state-dependent inactivation (*5*, *7*, *9*). This mechanism relies on receptors becoming inactivated (that is, they are no longer able to signal) after sensing the ligand by, for example, receptor down-regulation. Perfect adaptation is observed when all of the receptors are down-regulated (Fig. 1A) or if all of the ligand is removed by the down-regulation of receptor-ligand complexes (Fig. 1B).

The conditions for perfect adaptation exhibited by other receptors are not readily applicable to the TCR. First, complete down-regulation of the TCR is not commonly observed nor is it required for T cell activation (*10*–*14*). Second, the complete removal of the pMHC ligand has not been reported, although there are reports that some pMHCs can be internalized by T cells (*15*). Instead, individual pMHC ligands can serially engage and down-regulate many TCRs (*16*) and, on the time scale of hours, they can sustain TCR signaling to induce digital cytokine production (*17*). Although TCR down-regulation does not appear to meet the criteria for perfect adaptation, it has been suggested to play an important physiological role in peripheral tolerance (*18*–*22*). This concept is supported by studies showing that defects in TCR down-regulation lead to hyperresponsive T cells with a loss of tolerance to persistent self-antigens, which results in autoimmune phenotypes (*23*–*27*), and that this is associated with sustained early TCR signaling (*28*, *29*). However, studies in which transgenic mice were challenged with peripheral antigens came to inconsistent conclusions, with some investigators reporting

[1]Sir William Dunn School of Pathology, University of Oxford, OX1 3RE Oxford, UK. [2]Radcliffe Department of Medicine, Medical Research Council Human Immunology Unit, Weatherall Institute of Molecular Medicine, University of Oxford, OX1 3RE Oxford, UK. [3]Electrical and Computer Engineering and Bioengineering, Northeastern University, Boston, MA 02115, USA.
*These authors contributed equally to this work.
†Present address: McKinsey & Company Christophstraße 17 50670 Köln Germany.
‡Present address: Novartis Pharma GmbH Roonstraße 25 90429 Nürnberg.
§Present address: Department of Chemical Engineering, Massachusetts Institute of Technology, Cambridge, MA 02139, USA.
||Corresponding author. Email: omer.dushek@path.ox.ac.uk

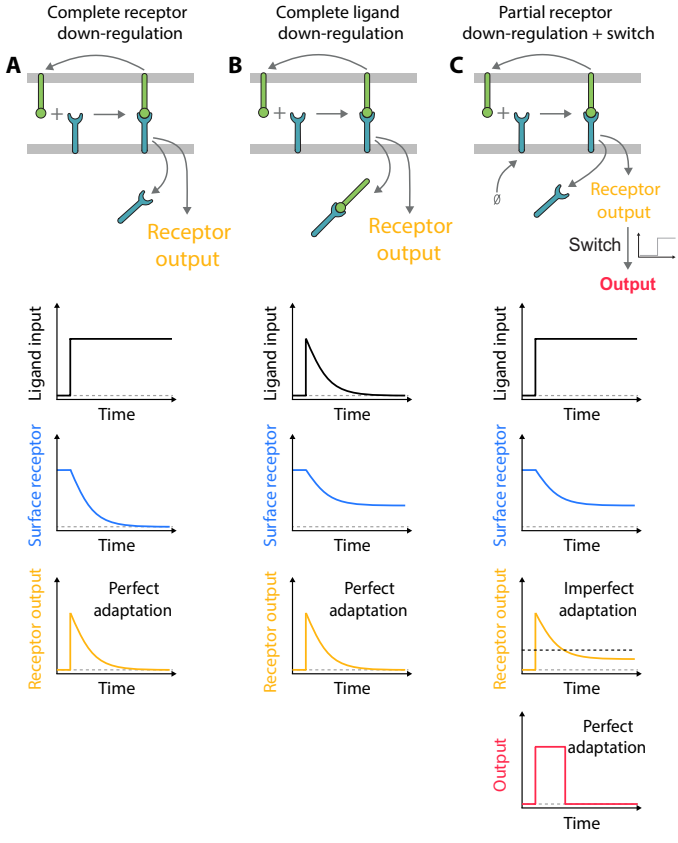

Fig. 1. Mechanisms of perfect adaptation based on receptor down-regulation. (**A**) Perfect adaptation can be observed if the ligand induces the down-regulation of all of the receptors. This mechanism requires that the reexpression of the receptor on the surface is negligible on the time scale of adaptation. (**B**) Alternatively, perfect adaptation can also be observed with partial receptor down-regulation if all of the ligand is removed by the down-regulation of receptor-ligand complexes. This mechanism requires that the receptors are in excess of the ligand (shown) or that receptors are reexpressed on the adaptation time scale (not shown) so that all of the ligand is removed. (**C**) Receptor output exhibits imperfect adaptation in the model in (A) if the receptor is replenished at the cell surface. In this case, perfect adaptation can be observed if a switch is introduced downstream of the receptor (threshold indicated by the dashed horizontal line). In all schematics, the ligand input represents the concentration of ligand available to bind to the receptor (not including internalized ligand). The mechanism of adaptation by receptor down-regulation is a subset of the more general mechanism of state-dependent inactivation (*5*, *9*), which is effectively an IFFL (*7*).

near-complete TCR down-regulation as the mechanism of tolerance (*20*, *30*–*33*), whereas others concluded that TCR down-regulation did not play a role in tolerance because overt down-regulation was not observed (*34*–*38*). Therefore, it would seem that complete TCR down-regulation is not necessary for adaptation tolerance (*3*). Maintaining T cell responses is critical in adoptive therapies in which T cells produced by in vitro expansion are transferred into patients with cancer and migrate into tumor microenvironments with chronic cancer antigens (*39*). These T cells are often armed with affinity-enhanced TCRs or synthetic chimeric antigen receptors (CARs) that redirect them to tumor cell antigens. Similarly to TCRs, CARs are down-regulated as a function of antigen concentration, and T cells with lower CAR surface abundance are less responsive than those with greater surface amounts of CAR (*40*–*44*). How CAR and TCR down-regulation shapes the response of these clinically relevant T cells is poorly understood.

Here, we investigated how constant stimulation with antigen regulated the responses of clinically relevant, in vitro–expanded primary human $CD8^+$ T cells. We observed perfect (or near-perfect) adaptation in cytokine production over a 100,000-fold variation in antigen affinity with partial TCR down-regulation. Mathematical modeling showed that TCR down-regulation produced imperfect adaptation but, when coupled to a switch, led to perfect adaptation (Fig. 1C). This model predicted that TCR down-regulation reduced, but did not abolish, TCR signaling below the threshold for sustained cytokine production. Consistent with this prediction, we showed that CD28 and 4-1BB costimulation reactivated T cell cytokine production in a pMHC-dependent manner. Last, we showed that adaptation was partially avoided in CAR-T cells that incorporated costimulatory domains within the synthetic receptor. Therefore, adaptation can substantially limit the production of cytokines in adoptive transfer therapies and has important implications for the design of adaptation-resistant TCR and CAR constructs.

RESULTS

Perfect adaptation of T cell responses to constant antigen over large variations in concentration and affinity

Using a standard adoptive therapy protocol (*45*), we generated in vitro–expanded primary human $CD8^+$ T cells expressing the therapeutic affinity-enhanced c58c61 TCR (*46*), which recognizes the NY-ESO-$1_{157\text{-}165}$ cancer testes antigen peptide bound to human leukocyte antigen–A2 (HLA-A2; Fig. 2A; see Materials and Methods). To enable constant antigen presentation and to study the effects in isolation, the T cells were stimulated by recombinant pMHC ligands on plates (*47*–*49*). This system has been widely used to isolate the effects of specific ligands and to precisely control the duration of stimulation (*50*).

T cells stimulated by the high-affinity pMHC antigen 9V (K_D = 70.7 pM) exhibited perfect adaptation, with the secreted amounts of tumor necrosis factor–α (TNF-α) stabilizing by 4 hours (Fig. 2, B and C, left). This adaptation was observed at all antigen concentrations tested. Within this range, high concentrations induced an earlier decline in the rate of TNF-α secretion starting at 2 hours. This resulted in a bell-shaped dose-response curve, which was previously observed in this system (*47*) and in other experimental systems (*51*).

Given that this adaptation was observed with a supraphysiological antigen affinity, we could not exclude the possibility that it was an uncharacteristic response to an excessive antigen signal. We therefore repeated the experiment with a pMHC with physiological affinity (4A8K, K_D = 7.23 μM). Although a higher concentration was required to initiate TNF-α production, the adaptation phenotype was kinetically identical (Fig. 2, B and C, right). We also observed the adaptation phenotype for interleukin-2 (IL-2), macrophage inflammatory protein–1β (MIP-1β), and interferon-γ (IFN-γ; figs. S1 and S2). The constant amount of cytokine in the culture medium may be established by a balance between uptake and continued secretion, by a stop in secretion, or a combination of both. Using single-cell intracellular cytokine staining, we observed that fewer T cells stained positive for TNF-α beyond 3 hours after stimulation (fig. S3), suggesting that cytokine production stopped, consistent with a previous report (*52*). Together, these data suggest that perfect

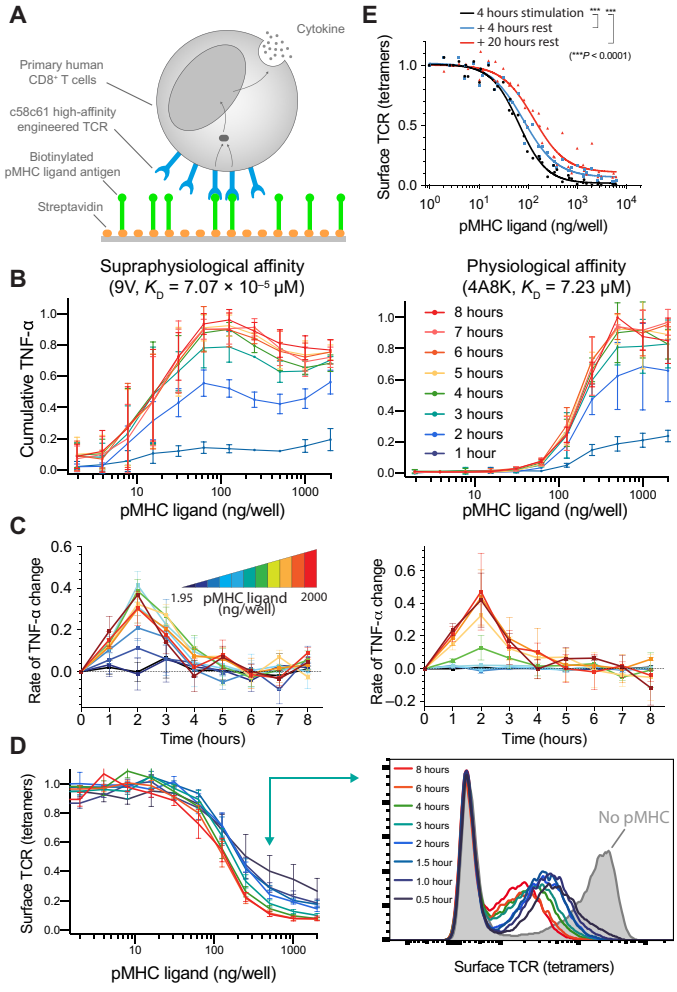

Fig. 2. Perfect adaptation of T cells to constant stimulation with pMHC ligand over large variations in affinity and concentration. (**A**) Primary human CD8$^+$ T cells expressing the c58c61 TCR were stimulated with recombinant pMHC immobilized on plates, as indicated. The amounts of cytokines secreted into the culture medium and the cell surface abundance of the TCR were measured (see Materials and Methods). (**B**) Cumulative TNF-α abundance over the concentration of 9V (left) or 4A8K (right) pMHC for 1 to 8 hours. Data are means and SD of three independent repeats. (**C**) Data from the experiments shown in (B) expressed as a rate of change of cumulative TNF-α. (**D**) Surface TCR expression measured using pMHC tetramers in flow cytometry for 4A8K (left) with a representative histogram (right). Data are means and SD of three independent repeats. Down-regulation could also be observed with TCR antibodies (fig. S4). (**E**) Recovery of surface TCR was measured by stimulating T cells for 4 hours to induce down-regulation (black line) followed by transfer to empty plates without pMHC for 4 (blue) or 20 (red) hours before measuring surface TCR abundance with pMHC tetramers. Combined data from all three independent experiments are shown. Expanded data showing the secretion of MIP-1β, IFN-γ, and IL-2, together with raw data before averaging are summarized in figs. S1 and S2, and single-cell intracellular cytokine staining data are shown in fig. S3.

adaptation in cytokine production was observed with similar temporal kinetics across a 2000-fold variation in antigen concentration and a 100,000-fold variation in antigen affinity.

Perfect adaptation cannot be explained by complete TCR down-regulation

Previously, it was shown that complete receptor down-regulation can produce perfect adaptation provided that the receptor is not reexpressed on the surface on the adaptation time scale (Fig. 1A). We therefore examined the surface dynamics of the TCR in our experimental system using flow cytometry. Consistent with previous reports (*16*, *18*, *53*–*55*), we observed concentration-dependent TCR down-regulation that reached steady state within 3 to 6 hours (Fig. 2D). In all of the conditions tested, the TCR was only partially down-regulated, and this was not a result of a fraction of T cells down-regulating their TCR (that is, digital down-regulation) because histograms showed that the entire population of TCR-transduced T cells reduced their TCR surface expression (that is, exhibited analog down-regulation; see Fig. 2D). Consistent with previous reports (*18*, *56*), we observed a small but significant recovery in TCR surface expression on the time scale of 4 hours (Fig. 2E, compare black to blue line), suggesting that partial down-regulation was maintained by a balance of reexpression. Together, these data suggest that perfect adaptation cannot be explained by complete down-regulation of the TCR.

Perfect adaptation by imperfect adaptation at the TCR coupled to a downstream switch

That the increased abundance of the TCR could be observed on the adaptation time scale suggested that TCR down-regulation would lead to imperfect adaptation (Fig. 1C). Therefore, additional mechanism(s) are required to produce perfect adaptation in cytokine production. Given that all-or-none signaling switches have been documented in the TCR signaling pathways (*17*, *57*–*59*) and that digital cytokine production has been reported (*17*), we hypothesized that a downstream digital switch could convert imperfect adaptation at the TCR into perfect adaptation in cytokine production (Fig. 1C).

We converted the schematic (Fig. 1C) into an ordinary-differential-equation (ODE) model and used Approximate Bayesian Computations coupled to Sequential Monte Carlo (ABC-SMC) (*60*) to directly fit the model to the surface TCR and cytokine data (see Materials and Methods). Given that the experimental data are derived from a heterogeneous population of T cells, the ABC-SMC method is particularly appropriate because it effectively simulates a population of T cells with potentially different values of the model parameters representing population heterogeneity (fig. S5). The model produced an excellent fit to the data (Fig. 3A, solid lines), suggesting that partial TCR down-regulation coupled to digital cytokine production is sufficient to explain perfect adaptation. By examining the time course at a single concentration (Fig. 3B), it was observed that incomplete TCR down-regulation (*R*, surface TCR) led to imperfect adaptation in TCR/pMHC complexes (*C*, receptor output). Perfect adaptation in cytokine production (*O*, output) was observed in the model because the concentration of TCR/pMHC complexes decreased below the switch threshold required to maintain the output.

This mechanism predicts that increasing the antigen strength would induce further TCR down-regulation and cytokine production. Therefore, the model was used to predict the outcome of increasing the antigen affinity (fig. S6), and experiments confirmed that TCR amounts were tuned to the increased antigen strength with further cytokine production. As expected, reducing the antigen strength by reducing antigen affinity did not lead to marked changes in TCR expression or further cytokine production (fig. S6D, light purple line). In summary, and in contrast to adaptation by other receptors, perfect adaptation can be explained here by imperfect adaptation at the TCR by partial down-regulation coupled to a switch in the pathway for cytokine production (Fig. 1C).

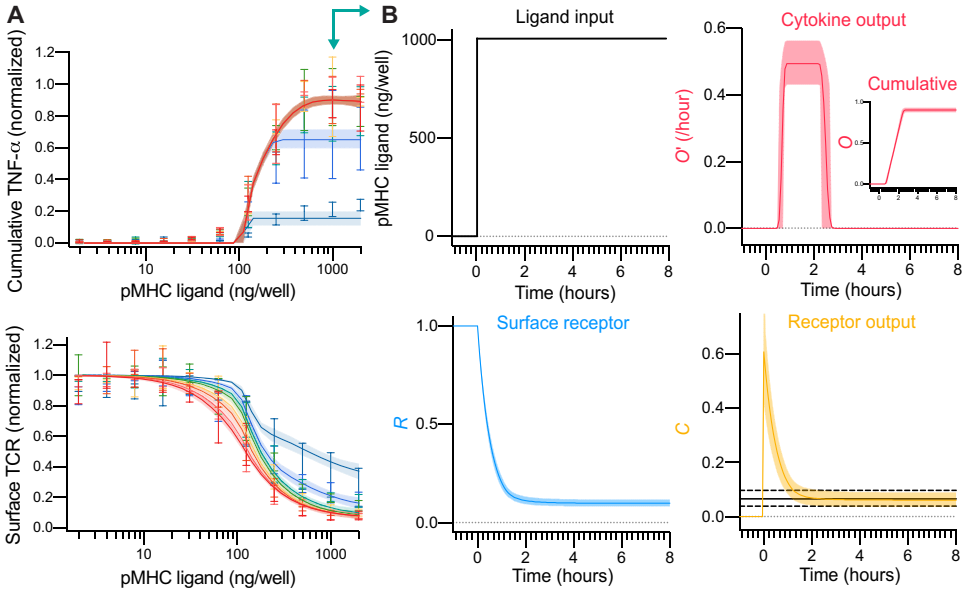

Fig. 3. A mechanistic mathematical model shows that TCR down-regulation coupled to a downstream switch is sufficient to explain perfect adaptation in T cell cytokine production to constant pMHC ligand stimulation. (**A**) The fit of the mathematical model (Fig. 1C) using ABC-SMC to analyze the physiological affinity pMHC data (Fig. 2, B and D). The solid line and the shaded region indicate the mean and the 95% confidence interval (CI) of the fit, respectively. (**B**) Model outputs over time for a single concentration [1000 ng per well, teal arrow in (A)]. The solid and dashed horizontal black lines in receptor output (bottom right) indicate the fitted mean threshold and 95% CIs, respectively, for the downstream switch. Distributions of all fitted parameters can be found in fig. S5.

T cell adaptation to constant pMHC antigen can be overridden by costimulation

The model predicted imperfect adaptation by TCR down-regulation so that residual TCR output continued after cytokine production had stopped (Fig. 3B). Given that T cells can encounter antigen in vivo in the context of costimulation through other surface receptors, and given that costimulation is thought to lower the signaling threshold for cytokine production (*61*–*63*), we determined whether costimulation could amplify residual TCR signaling to reactivate adapted T cells.

We used the mathematical model to predict the outcome of transferring T cells from a first stimulation to a second stimulation on the same antigen with or without costimulation (Fig. 4A). Note that in these transfer experiments, T cells experience the same concentration of antigen in the first and second stimulations. The effect of costimulation was simulated by lowering the switch threshold, and as expected, this enabled T cells to produce cytokine provided that they also continued to receive constant antigen stimulation (Fig. 4B). We note that similar results would be obtained if costimulation acted to increase TCR signaling but not if costimulation acted after the switch.

To test whether CD28 costimulation could override adaptation, we stimulated T cells with the physiological affinity pMHC (first stimulation) before transferring the cells to the same titration of pMHC with or without recombinant CD86, which is the ligand for CD28 (second stimulation). Consistent with the adaptation phenotype, there was a marked reduction in TNF-α production in the second stimulation without CD86; however, when CD86 was present, strong cytokine production was observed (Fig. 4C). Furthermore, T cells transferred to empty wells without pMHC or to wells coated with only CD86 produced no cytokines. In addition to CD28, the costimulatory receptor 4-1BB is also known to play an important role in the activation of $CD8^+$ T cells. We repeated the experiments with the recombinant ligand to 4-1BB, showing that this TNF receptor was also able to override adaptation but that, as with CD28, it critically relied on TCR/pMHC interactions (Fig. 4D). Costimulation through both CD28 and 4-1BB did not result in increased TCR surface expression (fig. S8).

Previous work on T cell anergy has described unresponsive T cell states that are induced when T cells are activated in the absence of CD28 costimulation. We therefore tested whether CD28 costimulation could prevent adaptation. We repeated the CD28 costimulation transfer experiments, but now transferred T cells that were stimulated with either pMHC alone or with both pMHC and CD86 in the first stimulation to a second stimulation that included pMHC alone, CD86 alone, pMHC and CD86, or empty wells. We observed reduced cytokine production in the second stimulation to pMHC alone, which was similar to the effect in empty wells, irrespective of whether CD86 was included in the first stimulation (fig. S9), suggesting that CD28 costimulation cannot prevent adaptation to constant antigen. Together, these results indicate that perfect adaptation in cytokine production induced by constant pMHC antigen stimulation does not lead to perfect adaptation in TCR signaling because extrinsic costimulation through CD28 or 4-1BB can induce adapted T cells to produce TNF-α in a pMHC-dependent manner. This phenotype was also observed for other cytokines (figs. S7 to S9).

Adaptation by CAR-T cells to constant antigen can be overridden by costimulatory domains

Given that CAR-T cells experience constant antigen stimulation in vivo, we analyzed their adaptation phenotype. To do this, we used the previously described T1 CAR (*64*) fused to the cytoplasmic tail of the ζ chain (first-generation CAR) that also recognizes the NY-ESO-$1_{157\text{-}165}$ peptide on HLA-A2 in a similar orientation to the TCR (K_D = 4 nM) (*65*). These CAR-T cells were first stimulated with a titration of 9V pMHC before being transferred for a second stimulation on the same titration of 9V (Fig. 5A). We observed reduced cytokine production by CAR-T cells that experienced the antigen in the first stimulation compared with that by CAR-T cells that were directly placed on the second stimulation (Fig. 5B, purple and orange lines, respectively). Given that costimulation can override adaptation, we repeated the experiments with a second-generation CAR containing the CD28 costimulatory domain and found that these CAR-T cells were able to partially avoid adaptation (Fig. 5C). Compared with the cytokine production observed after the first stimulation (100%), the production of TNF-α and IL-2 were reduced in the second stimulation to 26% (P = 0.0002) and 2.1%

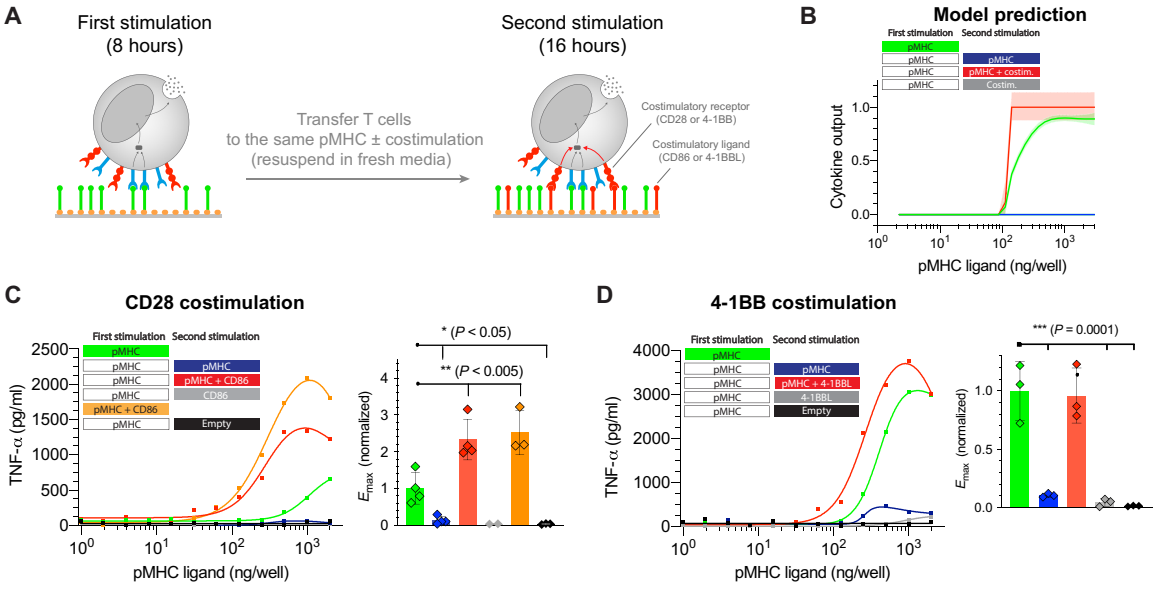

Fig. 4. Adapted T cells can be reactivated by CD28 or 4-1BB costimulation. (**A**) Schematic of the experiment showing that T cells were first stimulated for 8 hours before being transferred for a second stimulation for 16 hours with antigen alone, costimulation alone, or both antigen and costimulation. (**B**) Predicted cytokine production by the mathematical model where costimulation is assumed to lower the threshold for the downstream switch. (**C**) Representative TNF-α production (left) when providing costimulation to CD28 by recombinant biotinylated CD86 and averaged E_{max} values with SD from four independent experiments (right). (**D**) Representative TNF-α production (left) when providing costimulation to 4-1BB by recombinant biotinylated trimeric 4-1BBL and averaged E_{max} values with SD from three independent experiments (right). Statistical significance was determined by ordinary one-way ANOVA corrected for multiple comparisons by Dunnett's test. Expanded data showing additional cytokines and TCR down-regulation are shown in figs. S7 to S9.

($P = 0.002$) in the case of cells expressing the first-generation CAR but were only reduced to 58.7% ($P = 0.001$) and 79% ($P = 0.0031$) in cells expressing the second-generation CAR (Fig. 5, D and E). The ability of the second-generation CAR to resist adaptation was not a result of higher expression or an ability to resist down-regulation because this CAR was consistently expressed at lower amounts and down-regulated to a similar extent compared with the first-generation CAR (fig. S10).

Together, the adaptation phenotype observed with the TCR could also be observed with a first-generation CAR, which could be partially overridden by a second-generation CAR in the context of costimulation. Partial rescue in the case of the second-generation CAR was not unexpected because unlike the complete rescue of the TCR by extrinsic costimulation (Fig. 4), costimulation in the CAR is receptor intrinsic and is therefore reduced over time as a result of CAR down-regulation.

DISCUSSION

Using a reductionist system to provide T cells with constant pMHCs, we observed that in vitro–expanded primary human $CD8^+$ T cells did not maintain cytokine production but instead exhibited perfect adaptation across a 100,000-fold variation in antigen affinity. Their responses could be rescued by higher antigen affinity (fig. S6) or by costimulation (Fig. 4).

The constant amount of cytokine in the culture medium appeared consistent with a stop in production, secretion, or both rather than a balance between secretion and uptake/breakdown or activation-induced T cell death. First, intracellular cytokine staining showed fewer cytokine-positive T cells as stimulation times approached 8 hours (fig. S3). We noted that these single-cell experiments and the population-level cytokine secretion experiments (figs. S1 and S2) showed that IFN-γ appeared to exhibit delayed adaptation compared with other cytokines. This distinct behavior for IFN-γ could result from a subset of T cells being preprogrammed to produce it only after producing TNF-α (*66*). Second, continued secretion with balanced uptake would predict that replacing the medium would lead to detection of additional cytokine as the constant amount of cytokine in the medium is restored, but this was not observed in the transfer experiments (for example, Fig. 4, C and D, and figs. S7 and S9). These transfer experiments also highlight that the mechanism of adaptation is unlikely to be a result of complete removal of the pMHC ligand (Fig. 1B) because transferring T cells after they had adapted to plates newly coated with pMHC did not reactivate them to produce cytokine (for example, Fig. 4, C and D, and figs. S7 and S9). Last, activation-induced T cell death is unlikely because we previously confirmed that cell death is minimal in this experimental system (less than 10% of T cells stain positive for annexin V at 8 hours) (*47*), and second, adapted T cells were fully reactivated by costimulation (Fig. 4, C and D).

Mechanism of adaptation

Adaptation by surface receptors has been termed state-dependent inactivation (*5*, *9*), which is an IFFL whereby ligand binding induces receptor signaling (positive regulation) and receptor down-regulation (negative regulation) (*7*). Perfect adaptation occurs if the receptor is completely inactivated or down-regulated by the ligand. Unlike other receptors, the TCR is only partially down-regulated, leading to imperfect adaptation. To explain perfect adaptation in cytokine production, an additional downstream mechanism is required, and,

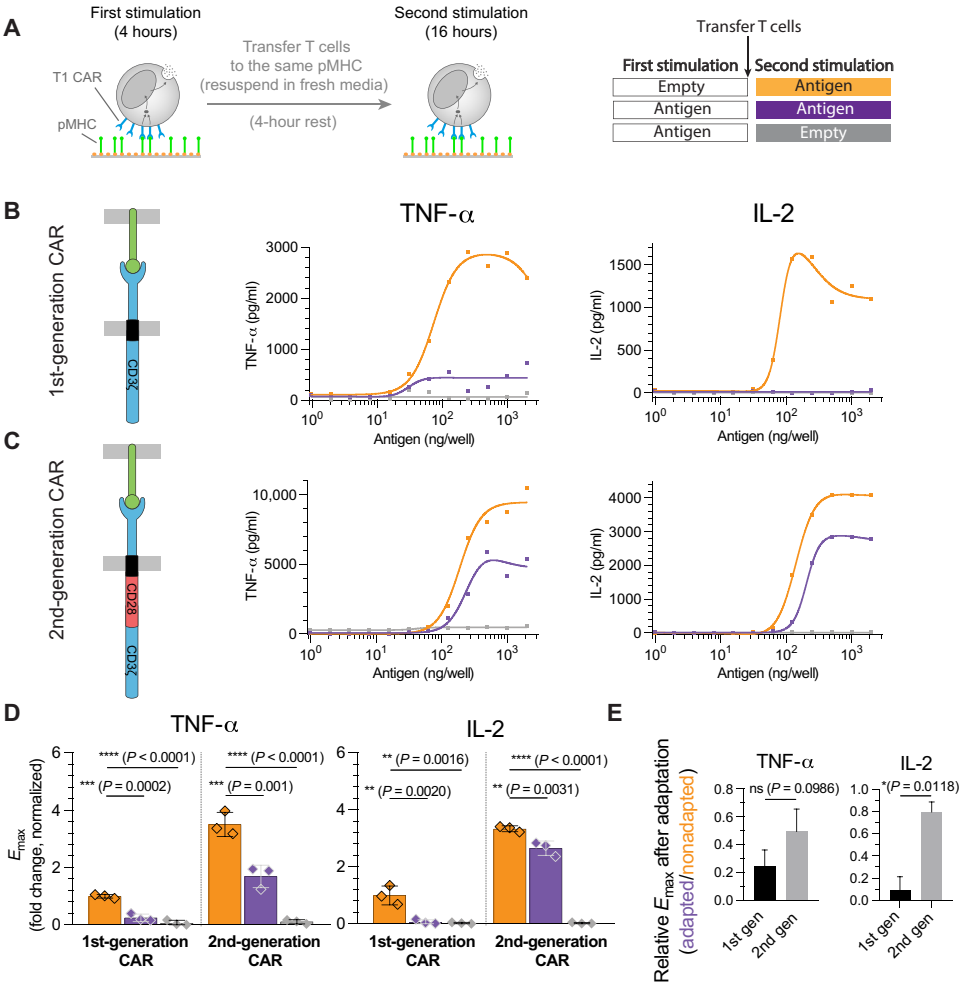

Fig. 5. Adaptation is partially avoided in the second- but not first-generation CAR-T cells. (**A**) Schematic of the experiment. T cells expressing the T1 CAR that recognizes the 9V pMHC antigen were transferred to the same titration of antigen. (**B** and **C**) Representative TNF-α and IL-2 production over antigen concentration from CAR-T cells expressing (B) the first-generation variant containing only the ζ chain and (C) the second-generation variant containing the cytoplasmic tail of CD28 fused to the ζ chain. (**D**) Averaged E_{max} values and SD for TNF-α (left) and IL-2 (right) three independent experiments. (**E**) Fold reduction in E_{max} between the first and second stimulation for the first- and second-generation CARs. The expression profile of both CARs and antigen-induced CAR down-regulation is shown in fig. S10. Statistical significance was determined by ordinary one-way ANOVA corrected for multiple comparisons by Dunnett's test. ns, not significant.

in the present study, we have invoked a switch (Fig. 1C). However, other signaling modules, such as additional IFFLs or NFLs, can also convert imperfect adaptation at the TCR to perfect adaptation in cytokine production.

The observation that 4-1BB costimulation could reactivate adapted T cells suggests that the identity of the additional downstream mechanism is likely to be at the transcriptional level. 4-1BB signaling activates nuclear factor κB (NF-κB) and mitogen-activated protein kinase (MAPK) pathways and is not known to interfere with TCR-proximal signaling. Moreover, TCR signaling results in the efficient and sustained nuclear translocalization of NFAT through Ca^{2+} signaling, whereas its ability to activate AP-1 and NF-κB without costimulation is relatively poor (*67*–*69*). The dependence of sustained cytokine production on these transcription factors suggests that T cells that adapted to the pMHC stimulus by down-regulating TCR signaling can be reactivated by 4-1BB costimulation because it is able to mitigate the lack of active AP-1 and NF-κB. Conversely, CD28 costimulation can modulate TCR proximal signaling, which may effectively amplify residual TCR signaling to restore the activation of AP-1 and NF-κB (*70*, *71*).

The minimal model of TCR down-regulation coupled to a downstream switch can produce bell-shaped dose-response curves (fig. S6B). Previously, we argued that bell-shaped dose-response curves can be explained by IFFLs, but not by TCR down-regulation (*47*). The key assumption underlying this conclusion was that the rate of cytokine production was in steady state, which is the case for Jurkat cell lines (*47*), but the detailed analysis in the present work has revealed that it is not the case for primary T cells in the absence of costimulation. The bell-shaped dose-response curve produced by the kinetic model used here is a result of faster TCR down-regulation at higher antigen concentrations, resulting in cytokine production stopping at an earlier time point.

Function of adaptation

Adaptation is a critically important and widely implemented process in biology. Unlike for other receptors, perfect adaptation in T cells is achieved by imperfect adaptation at the TCR. This has the important consequence that adapted T cells are rendered dependent on both antigen and extrinsic costimulation. In the specific example of activated T cells, whose killing capacity is thought to be less dependent on costimulation, adaptation in cytokine production may be an important mechanism to ensure that their ability to initiate or maintain inflammation is extrinsically regulated by other cells. In this way, adaptation may serve to balance functional immunity with excessive tissue damage as was previously suggested (*3*, *72*).

Role of TCR down-regulation

T cells enter unresponsive states upon recognition of persistent self-antigens and viral antigens in vivo (*2*, *3*, *20*, *31*, *33*–*38*, *73*–*77*). Although the underlying mechanisms that induce and maintain these states are debated, their functional phenotype is characterized by transient cytokine production that can be overcome by costimulation as was observed here (Figs. 2 and 4). For example, effector $CD4^+$ T cells transiently produce cytokines despite continued antigen exposure (*76*), and the unresponsive (exhausted) phenotype of $CD8^+$ T cells induced by persistent antigens can be overcome by

costimulation (*77*). We note that the mechanism of adaptation that we report can take place with only minor TCR down-regulation, which may help reconcile previous reports arguing either that TCR down-regulation can explain tolerance (*20*, *30*–*33*) or that TCR down-regulation does not play a role in tolerizing T cells because overt down-regulation was not observed (*34*–*38*). In addition, our results suggest that adaptation by TCR down-regulation renders T cells dependent on costimulation, which is consistent with the finding that T cells with impaired TCR down-regulation lose their dependence on costimulation for activation (*25*, *27*). Ultimately, by studying in vitro–expanded human T cells, we are inherently limited in making direct comparisons with T cell phenotypes in vivo.

Implications for adoptive therapy

Consistent with the adaptation phenotype that we observed, CAR-T cells exposed to chronic antigen become unresponsive but can respond to a higher antigen concentration, which correlates with CAR expression (*43*). The ability of second-generation CARs to partially avoid adaptation in cytokine production (Fig. 5) may explain why they generate much more potent and persistent anti-tumor responses in vivo (*78*–*81*) although their in vitro killing capacity is comparable with those of cells expressing first-generation receptors (*79*–*82*). The optimization of TCRs and CARs has focused on affinity, cell surface abundance, and signaling potency, but engineering for optimal down-regulation has yet to be explored.

MATERIALS AND METHODS

Protein production

pMHCs were refolded in vitro from the extracellular residues 1 to 287 of the HLA-A*02:01 chain, β2-microglobulin, and NY-ESO-$1_{157\text{-}165}$ peptide variants as described previously (*47*). CHO (Chinese hamster ovary) cell lines permanently expressing the extracellular part of human CD86 (amino acid residues 6 to 247) with a His-tag for purification and a BirA biotinylation site were provided by S. Davis (Oxford, UK). Cells were cultured in glutamine synthetase selection medium [10% dialyzed fetal calf serum, 1× GSEM (Glutamine synthetase expression medium) supplement (Sigma-Aldrich), 20 to 50 μM MSX, and 1% penicillin-streptomycin] and passaged every 3 or 4 days. After four or five passages from thawing a new vial, cells from two confluent T175 flasks were transferred into a cell factory and incubated for 5 to 7 days, after which the medium was replaced. The supernatant was harvested after another 3 weeks, sterile filtered, and dialyzed overnight. The His-tagged CD86 was purified on a nickel–NTA (nitrilotriacetic acid agarose) column. 4-1BB ligand expression constructs were a gift from H. Wajant (Würzburg, Germany) and contained a Flag tag for purification and a tenascin-C trimerization domain. We added a BirA biotinylation site. The protein was produced by transient transfection of human embryonic kidney (HEK) 293T cells with XtremeGene HP Transfection reagent (Roche) according to the manufacturer's instructions and purified according to a published protocol (*83*), with the exception of the elution step, where we used acid elution with 0.1 M glycine-HCl (pH 3.5). The pMHC or costimulatory ligand was then biotinylated in vitro with BirA (Avidity) according to the manufacturer's instructions and purified by size exclusion chromatography.

Production of lentiviruses for transduction

HEK 293T cells were seeded into six-well plates 24 hours before undergoing transfection to achieve 50 to 80% confluency on the day of transfection. Cells were cotransfected with the respective third-generation lentiviral transfer vectors and packaging plasmids using Roche XtremeGene 9 (0.8 μg of lentiviral expression plasmid, 0.95 μg of pRSV-rev, 0.37 μg of pVSV-G, and 0.95 μg of pGAG). The supernatant was harvested and filtered through a 0.45-μm cellulose acetate filter 24 to 36 hours later. The 1G4 TCR used for this project was initially isolated from a patient with melanoma (*84*). The affinity maturation to the c58c61 TCR variant used herein was performed by Adaptimmune Ltd. The TCR and all CARs in this study have been used in a standard third-generation lentiviral vector with the EF1 promoter. The CAR constructs that bind the NY-ESO-$1_{157\text{-}165}$ HLA-A2 pMHC complex (*65*, *85*) were a gift from C. Renner (Zurich, Switzerland). The high-affinity T1 version was used for this project. All CAR constructs contained the scFv binding domain, a two-immunoglobulin domain spacer derived from an immunoglobulin G antibody Fc part, and the CD28 transmembrane domain. We modified the different CARs to contain the CD3ζ signaling domain alone or in combination with the CD28 signaling domain.

T cell isolation and culture

Up to 50 ml of peripheral blood was collected by a trained phlebotomist from healthy volunteer donors after informed consent had been taken. This project was approved by the Medical Sciences Inter-Divisional Research Ethics Committee of the University of Oxford (R51997/RE001), and all samples were anonymized in compliance with the Data Protection Act. Alternatively, leukocyte cones were purchased from the National Health Services Blood and Transplant service. Only HLA-$A2^-$ peripheral blood or leukocyte cones were used because of the cross-reactivity of the high-affinity receptors used in this study, which leads to the fratricide of HLA-$A2^+$ T cells (*64*, *65*, *86*). $CD8^+$ T cells were isolated directly from blood using the $CD8^+$ T Cell Enrichment Cocktail (StemCell Technologies) and density gradient centrifugation according to the manufacturer's instructions. The isolated $CD8^+$ T cells were washed and resuspended at a concentration of 1×10^6 cells/ml in completely reconstituted RPMI supplemented with IL-2 (50 U/ml) and 1×10^6 CD3/CD28-coated Human T-Activator Dynabeads (Life Technologies) per milliliter. The next day, 1×10^6 T cells were transduced with 2.5 ml of the virus-containing supernatant from one well of HEK cells supplemented with IL-2 (50 U/ml). The medium was replaced with fresh medium containing IL-2 (50 U/ml) every 2 to 3 days. CD3/CD28-coated beads were removed on day 5 after lentiviral transduction, and the cells were used for experiments on days 10 to 14. This protocol produces antigen-experienced $CD8^+$ T cells, with a fraction (typically ~70%) expressing the transduced c58c61 TCR or T1 CAR.

T cell stimulation

T cells were stimulated with titrated amounts of plate-immobilized pMHC ligands with or without coimmobilized ligands for accessory receptors. Ligands were diluted to the working concentrations in sterile phosphate-buffered saline (PBS). Fifty microliters of serially twofold diluted pMHC was added to each well of streptavidin-coated 96-well plates (15500, Thermo Fisher Scientific). After a minimum of 45 min of incubation, the plates were washed once with sterile PBS. Where accessory receptor ligands were used, those were similarly diluted and added to the plate for a second incubation of 45 to 90 min. In experiments with small-molecule inhibitors, the T cells were incubated with the inhibitor at 37°C for 20 to 30 min before

the start of the stimulation. The inhibitors were left in the medium for the whole duration of the stimulation. All control conditions were incubated with dimethyl sulfoxide (DMSO) at a 1:1000 dilution so that the DMSO concentration was the same for the inhibitor and noninhibitor samples. PP2 was used at a final concentration of 20 μM. After washing the stimulation plate with PBS, 7.5×10^4 T cells were added in 200 μl of complete RPMI without IL-2 to each stimulation condition. The plates were spun at 9*g* for 2 min to settle down the cells and then incubated at 37°C in 5% CO_2. For transfer experiments, the T cells were pipetted from the stimulation plate into a V-bottom plate and pelleted after the first round of stimulation. The supernatant was stored at −20°C for later cytokine enzyme-linked immunosorbent assays (ELISAs), and the cells were resuspended in 200 μl of fresh R10 medium and, depending on the experiment, either rested for some time or transferred to another stimulation plate with a new set of conditions. The cells were then again settled down by centrifugation at 9*g* before incubation.

Flow cytometry

Flow cytometry was used to assess cell surface receptor expression after transduction of cells with TCR and CAR constructs and to quantify receptor down-regulation at the end of the stimulation experiments. After stimulation, T cells were pelleted in a V-bottom plate and resuspended in 40 μl of PBS with 2% bovine serum albumin and fluorescent 9V pMHC tetramers conjugated with streptavidin-phycoerythrin (BioLegend, 405204) and used at a predetermined dilution (1:100 to 1:1000). The staining mixture was incubated for 20 to 60 min, after which the cells were pelleted, resuspended in 70 to 100 μl of PBS, and analyzed on a FACSCalibur or LSRFortessa X-20 (BD) flow cytometer. Flow cytometry data were analyzed with Flowjo V10.0 software.

ELISA

Supernatants from stimulation experiments were stored at −20°C. Cytokine concentrations were measured by ELISAs according to the manufacturer's instructions in Nunc MaxiSorp flat-bottom plates (Invitrogen) using Uncoated ELISA Kits (Invitrogen) for TNF-α, IFN-γ, MIP-1β, and IL-2.

Data analysis

The fraction of T cells expressing the transduced TCR or CAR and the amount of cytokine in the culture medium exhibited variation between independent experiments (with different donors). Therefore, directly averaging the data produced curves that were not representative of individual repeats. To average the cytokine data, the maximum for each repeat was normalized to 1 before averaging independent repeats. To average surface TCR geometric mean fluorescence intensity (gMFI; *X*), which is on a logarithmic scale, we used the following formula that corrected for the fraction of T cells expressing the TCR(f): $(X/X_0^{1-f})^{1/f}$, where X_0 is the mean background gMFI of the TCR-negative population. After applying this transform, each repeat was normalized to the maximum gMFI before averaging independent repeats. The statistical analysis of maximum cytokine produced across different pMHC concentrations (E_{max}) was performed by expressing E_{max} as a fold change to pMHC alone before averaging independent repeats. Given that the dose-response curves often exhibited a bell shape, it was not possible to use a standard Hill function to estimate E_{max}. Instead, we used lsqcurvefit in Matlab (MathWorks) to fit a function that was the difference of two Hill curves to generate a smooth spline through the data from which the maximum value of cytokine was estimated. This procedure was used to extract E_{max} values in Figs. 4 and 5 and figs. S7 and S9. In a limited number of cases, individual outlier values were excluded before data fitting but are still shown as data points in the respective figures.

Statistical analysis

Ordinary one-way analysis of variance (ANOVA) corrected for multiple comparisons by Dunnett's test was performed on the experimental data to determine statistical significance for Figs. 4 (C and D) and 5 (D and E), and figs. S6C and S9. Statistical significance for surface TCR recovery (Fig. 2E) was performed by using an *F* test for the null hypothesis that a single Hill curve (with the same parameters) can explain the data. GraphPad Prism software was used for all statistical analyses.

Mathematical model

The mathematical model (Fig. 1C) is represented as a system of two nonlinear coupled ODEs

$$\frac{dR}{dt} = k_1(1-R) - k_3 C - k_2 H(C-K_2)R$$

$$\frac{dO}{dt} = k_4 H(C-K_4) H(t-t_{delay})$$

where *R* and *O* are the surface TCR amounts (normalized to 1) and cumulative cytokine output with initial conditions 1 and 0, respectively. Given that TCR/pMHC binding kinetics (seconds) are faster than experimental time scales (hours), the concentration of TCR/pMHC complexes (*C*, defined as receptor output) was assumed to be in quasi–steady state: $C(t) = L^n R(t)/(K_0^n + L^n)$, where *L* is the given concentration of pMHC (in nanogram per well scale), K_0 is the effective dissociation constant (in nanogram per well scale), and *n* is the Hill number. In the equation for *R*, the first two terms are the basal turnover of surface TCR ($k_1(1-R)$) and the pMHC binding induced down-regulation of TCR ($-k_3C$). In the equation for *O*, the term for the switch [$k_4H(C-K_4)$] includes a Heaviside step function (H), so that the term is 0 unless receptor output (C) is above the switch threshold (K_4), and in this case, cytokine output is produced at rate k_4. To directly fit the model to the data, two additional modifications were required. First, TCR down-regulation is biphasic in time (*54*, *56*) (for example, see Fig. 2D), requiring an additional term for down-regulation in the equation for *R* [$k_2H(C-K_2)R$]. This term increases TCR down-regulation initially when the output from the receptor (C) is above a threshold (K_2), and at a molecular level, this may represent signaling-dependent bystander down-regulation (*13*). Given that the model already contained a stiff step function in the equation for *O*, this step function was approximated by a Hill number with large cooperativity for computational efficiency [$k_2H(C-K_2) \approx k_2 \frac{C^s}{K_2^s + C^s}$, $s = 12$]. Second, cytokine production was larger in the second hour compared with that in the first hour (for example, see Fig. 2B), which may be associated with transcriptional delays. To capture this delay, a multiplicative term in the equation for *O* was introduced [$H(t-t_{delay})$] so that cytokine production was only initiated after a delay of t_{delay}.

Data fitting using ABC-SMC

A Matlab (MathWorks) implementation of a previously published algorithm for ABC-SMC was used for data fitting (*60*). The ODEs

were evaluated using the Matlab function ode23s. Using ABC-SMC, the values of $R(t)$ and $O(t)$ were directly fitted to the normalized surface TCR levels and cumulative cytokine output, respectively, for the dose-response time course of 4A8K (192 data points in total). The distance measure was the standard sum-squared residuals, and all nine model parameters were fitted (K_0, n, k_1, k_2, K_2, k_3, k_4, K_4, and t_{delay}). A population of 3000 particles was initialized with uniform priors in log space and propagated through 30 populations, by which point the distance measure was no longer decreasing. The final population of 3000 particles, each of which had a different set of model parameters (fig. S5), was used to display the quality of the fit (Fig. 3A). Although the ODE model represents the reactions within a single cell and, hence, the dose-response curve for a single cell would exhibit a perfect switch (that is, a step function), the population-averaged dose-response curves from the model include particles (that is, cells) with different parameter values, accounting for population heterogeneity, leading to a more gradual dose-response curve. The posterior distributions revealed that only a subset of the model parameters was uniquely determined (fig. S5). Nonetheless, we were still able to make predictions using the model by simulating different experimental conditions for the 3000 particles in the final population. To predict the effect of increasing antigen affinity (fig. S6B), the TCR/pMHC binding parameters in the model (K_0 and n) for each particle were reduced by 50%. To predict the effect of costimulation (Fig. 4B), the threshold for the switch (K_2) for each particle was reduced by 60% for a duration of 8 hours. The value of 60% was chosen because it approximately reproduced the EC_{50} (half-maximal effective concentration) of ~100 ng per well observed in the data. The duration of this reduction scaled the value of E_{max}.

SUPPLEMENTARY MATERIALS

stke.sciencemag.org/cgi/content/full/14/666/eaay9363/DC1

Fig. S1. Cytokine production by T cells in response to constant stimulation by the supraphysiological affinity pMHC 9V.

Fig. S2. Cytokine production by T cells in response to constant stimulation by the physiological affinity pMHC 4A8K.

Fig. S3. T cell adaptation is the result of reduced cytokine production per cell.

Fig. S4. Quantitative assessment of TCR down-regulation is independent of the detection method used.

Fig. S5. Posterior distributions of 3000 particles after 30 populations using ABC-SMC.

Fig. S6. T cells adapted to a low-affinity antigen can be reactivated with a higher-affinity antigen.

Fig. S7. T cells adapted to constant antigen can be reactivated with 4-1BB costimulation.

Fig. S8. Costimulation by CD28 and 4-1BB does not increase TCR surface expression after adaptation.

Fig. S9. CD28 costimulation does not prevent adaptation to constant antigen stimulation.

Fig. S10. Expression levels and antigen-induced down-regulation of first- and second-generation CARs.

View/request a protocol for this paper from *Bio-protocol*.

REFERENCES AND NOTES

1. J. E. Smith-Garvin, G. A. Koretzky, M. S. Jordan, T cell activation. *Annu. Rev. Immunol.* **27**, 591–619 (2009).
2. M. Hashimoto, A. O. Kamphorst, S. J. Im, H. T. Kissick, R. N. Pillai, S. S. Ramalingam, K. Araki, R. Ahmed, CD8 T cell exhaustion in chronic infection and cancer: Opportunities for Interventions. *Annu. Rev. Med.* **69**, 301–318 (2018).
3. R. H. Schwartz, T cell anergy. *Annu. Rev. Immunol.* **21**, 305–334 (2003).
4. A. Alcover, B. Alarcón, V. D. Bartolo, Cell biology of T cell receptor expression and regulation. *Annu. Rev. Immunol.* **36**, 103–125 (2018).
5. J. E. Ferrell, Perfect and near-perfect adaptation in cell signaling. *Cell Syst.* **2**, 62–67 (2016).
6. W. Ma, A. Trusina, H. el-Samad, W. A. Lim, C. Tang, Defining network topologies that can achieve biochemical adaptation. *Cell* **138**, 760–773 (2009).
7. S. J. Rahi, J. Larsch, K. Pecani, A. Y. Katsov, N. Mansouri, K. Tsaneva-Atanasova, E. D. Sontag, F. R. Cross, Oscillatory stimuli differentiate adapting circuit topologies. *Nat. Methods* **14**, 1010–1016 (2017).
8. H. Shankaran, H. Resat, H. S. Wiley, Cell surface receptors for signal transduction and ligand transport: A design principles study. *PLOS Comput. Biol.* **3**, e101 (2007).
9. T. Friedlander, N. Brenner, Adaptive response by state-dependent inactivation. *Proc. Natl. Acad. Sci.* **106**, 22558–22563 (2009).
10. A. Viola, A. Lanzavecchia, T cell activation determined by T cell receptor number and tunable thresholds. *Science* **273**, 104–106 (1996).
11. Z. Cai, H. Kishimoto, A. Brunmark, M. R. Jackson, P. A. Peterson, J. Sprent, Requirements for peptide-induced T cell receptor downregulation on naive CD8 T cells. *J. Exp. Med.* **185**, 641–652 (1997).
12. M. Salio, S. Valitutti, A. Lanzavecchia, Agonist-induced T cell receptor down-regulation: Molecular requirements and dissociation from T cell activation. *Eur. J. Immunol.* **27**, 1769–1773 (1997).
13. E. S. José, A. Borroto, F. Niedergang, A. Alcover, B. Alarcón, Triggering the TCR complex causes the downregulation of nonengaged receptors by a signal transduction-dependent mechanism. *Immunity* **12**, 161–170 (2000).
14. A. Monjas, A. Alcover, B. Alarcón, Engaged and bystander T cell receptors are down-modulated by different endocytotic pathways. *J. Biol. Chem.* **279**, 55376–55384 (2004).
15. J.-F. Huang, Y. Yang, H. Sepulveda, W. Shi, I. Hwang, P. A. Peterson, M. R. Jackson, J. Sprent, Z. Cai, TCR-mediated internalization of peptide-MHC complexes acquired by T cells. *Science* **286**, 952–954 (1999).
16. S. Valitutti, S. Müller, M. Cella, E. Padovan, A. Lanzavecchia, Serial triggering of many T-cell receptors by a few peptide-Mhc complexes. *Nature* **375**, 148–151 (1995).
17. J. Huang, M. Brameshuber, X. Zeng, J. Xie, Q. J. Li, Y. H. Chien, S. Valitutti, M. M. Davis, A single peptide-major histocompatibility complex ligand triggers digital cytokine secretion in $CD4^+$ T cells. *Immunity* **39**, 846–857 (2013).
18. E. L. Reinherz, S. Meuer, K. A. Fitzgerald, R. E. Hussey, H. Levine, S. F. Schlossman, Antigen recognition by human T lymphocytes is linked to surface expression of the T3 molecular complex. *Cell* **30**, 735–743 (1982).
19. E. D. Zanders, J. R. Lamb, M. Feldmann, N. Green, P. C. L. Beverley, Tolerance of T-cell clones is associated with membrane antigen changes. *Nature* **303**, 625–627 (1983).
20. G. Schönrich, U. Kalinke, F. Momburg, M. Malissen, A. M. Schmitt-Verhulst, B. Malissen, G. J. Hämmerling, B. Arnold, Down-regulation of T cell receptors on self-reactive T cells as a novel mechanism for extrathymic tolerance induction. *Cell* **65**, 293–304 (1991).
21. S. Cemerski, J. Das, E. Giurisato, M. A. Markiewicz, P. M. Allen, A. K. Chakraborty, A. S. Shaw, The balance between T cell receptor signaling and degradation at the center of the immunological synapse is determined by antigen quality. *Immunity* **29**, 414–422 (2008).
22. A. M. Gallegos, H. Xiong, I. M. Leiner, B. Sušac, M. S. Glickman, E. G. Pamer, J. W. J. van Heijst, Control of T cell antigen reactivity via programmed TCR downregulation. *Nat. Immunol.* **17**, 379–386 (2016).
23. M. A. Murphy, R. G. Schnall, D. J. Venter, L. Barnett, I. Bertoncello, C. B. F. Thien, W. Y. Langdon, D. D. L. Bowtell, Tissue hyperplasia and enhanced T-cell signaling via ZAP-70 in c-Cbl-deficient mice. *Mol. Cell. Biol.* **18**, 4872–4882 (1998).
24. M. Naramura, H. K. Kole, R. J. Hu, H. Gu, Altered thymic positive selection and intracellular signals in Cbl-deficient mice. *Proc. Natl. Acad. Sci. U.S.A.* **95**, 15547–15552 (1998).
25. K. Bachmaier, C. Krawczyk, I. Kozieradzki, Y. Y. Kong, T. Sasaki, A. Oliveira-dos-Santos, S. Mariathasan, D. Bouchard, A. Wakeham, A. Itie, J. le, P. S. Ohashi, I. Sarosi, H. Nishina, S. Lipkowitz, J. M. Penninger, Negative regulation of lymphocyte activation and autoimmunity by the molecular adaptor Cbl-b. *Nature* **403**, 211–216 (2000).
26. M. S. Jeon, A. Atfield, K. Venuprasad, C. Krawczyk, R. Sarao, C. Elly, C. Yang, S. Arya, K. Bachmaier, L. Su, D. Bouchard, R. Jones, M. Gronski, P. Ohashi, T. Wada, D. Bloom, C. G. Fathman, Y. C. Liu, J. M. Penninger, Essential role of the E3 ubiquitin ligase Cbl-b in T cell anergy induction. *Immunity* **21**, 167–177 (2004).
27. R. I. Nurieva, S. Zheng, W. Jin, Y. Chung, Y. Zhang, G. J. Martinez, J. M. Reynolds, S.-L. Wang, X. Lin, S.-C. Sun, G. Lozano, C. Dong, The E3 ubiquitin ligase GRAIL regulates T cell tolerance and regulatory T cell function by mediating T cell receptor-CD3 degradation. *Immunity* **32**, 670–680 (2010).
28. K.-H. Lee, A. R. Dinner, C. Tu, G. Campi, S. Raychaudhuri, R. Varma, T. N. Sims, W. R. Burack, H. Wu, J. Wang, O. Kanagawa, M. Markiewicz, P. M. Allen, M. L. Dustin, A. K. Chakraborty, A. S. Shaw, The immunological synapse balances T cell receptor signaling and degradation. *Science* **302**, 1218–1222 (2003).
29. M. Naramura, I.-K. Jang, H. Kole, F. Huang, D. Haines, H. Gu, c-Cbl and Cbl-b regulate T cell responsiveness by promoting ligand-induced TCR down-modulation. *Nat. Immunol.* **3**, 1192–1199 (2002).
30. I. Ferber, G. Schönrich, J. Schenkel, A. Mellor, G. Hammerling, B. Arnold, Levels of peripheral T cell tolerance induced by different doses of tolerogen. *Science* **263**, 674–676 (1994).

31. A. Tafuri, J. Alferink, P. Möller, G. J. Hämmerling, B. Arnold, T cell awareness of paternal alloantigens during pregnancy. *Science* **270**, 630–633 (1995).
32. S. Martin, M. J. Bevan, Transient alteration of T cell fine specificity by a strong primary stimulus correlates with T cell receptor down-regulation. *Eur. J. Immunol.* **28**, 2991–3002 (1998).
33. P. Stamou, J. de Jersey, D. Carmignac, C. Mamalaki, D. Kioussis, B. Stockinger, Chronic exposure to low levels of antigen in the periphery causes reversible functional impairment correlating with changes in CD5 levels in monoclonal CD8 T cells. *J. Immunol.* **171**, 1278–1284 (2003).
34. N. J. Singh, R. H. Schwartz, The strength of persistent antigenic stimulation modulates adaptive tolerance in peripheral $CD4^+$ T cells. *J. Exp. Med.* **198**, 1107–1117 (2003).
35. D. Hawiger, R. F. Masilamani, E. Bettelli, V. K. Kuchroo, M. C. Nussenzweig, Immunological unresponsiveness characterized by increased expression of CD5 on peripheral T cells induced by dendritic cells in vivo. *Immunity* **20**, 695–705 (2004).
36. K. R. Ryan, D. McCue, S. M. Anderton, Fas-mediated death and sensory adaptation limit the pathogenic potential of autoreactive T cells after strong antigenic stimulation. *J. Leukoc. Biol.* **78**, 43–50 (2005).
37. J. R. Lees, B. Charbonneau, A. K. Swanson, R. Jensen, J. F. Zhang, R. Matusik, T. L. Ratliff, Deletion is neither sufficient nor necessary for the induction of peripheral tolerance in mature $CD8^+$ T cells. *Immunology* **117**, 248–261 (2006).
38. S. Han, A. Asoyan, H. Rabenstein, N. Nakano, R. Obst, Role of antigen persistence and dose for $CD4^+$ T-cell exhaustion and recovery. *Proc. Natl. Acad. Sci. U.S.A* **107**, 20453–20458 (2010).
39. C. H. June, R. S. O'Connor, O. U. Kawalekar, S. Ghassemi, M. C. Milone, CAR T cell immunotherapy for human cancer. *Science* **359**, 1361–1365 (2018).
40. S. E. James, P. D. Greenberg, M. C. Jensen, Y. Lin, J. Wang, L. E. Budde, B. G. Till, A. A. Raubitschek, S. J. Forman, O. W. Press, Mathematical modeling of chimeric TCR triggering predicts the magnitude of target lysis and its impairment by TCR downmodulation. *J. Immunol.* **184**, 4284–4294 (2010).
41. H. G. Caruso, L. V. Hurton, A. Najjar, D. Rushworth, S. Ang, S. Olivares, T. Mi, K. Switzer, H. Singh, H. Huls, D. A. Lee, A. B. Heimberger, R. E. Champlin, L. J. N. Cooper, Tuning sensitivity of CAR to EGFR density limits recognition of normal tissue while maintaining potent antitumor activity. *Cancer Res.* **75**, 3505–3518 (2015).
42. S. Arcangeli, M. C. Rotiroti, M. Bardelli, L. Simonelli, C. F. Magnani, A. Biondi, E. Biagi, S. Tettamanti, L. Varani, Balance of anti-CD123 chimeric antigen receptor binding affinity and density for the targeting of acute myeloid leukemia. *Mol. Ther.* **25**, 1933–1945 (2017).
43. C. Han, S. J. Sim, S. H. Kim, R. Singh, S. Hwang, Y. I. Kim, S. H. Park, K. H. Kim, D. G. Lee, H. S. Oh, S. Lee, Y. H. Kim, B. K. Choi, B. S. Kwon, Desensitized chimeric antigen receptor T cells selectively recognize target cells with enhanced antigen expression. *Nat. Commun.* **9**, 468 (2018).
44. J. Eyquem, J. Mansilla-Soto, T. Giavridis, S. J. C. van der Stegen, M. Hamieh, K. M. Cunanan, A. Odak, M. Gönen, M. Sadelain, Targeting a CAR to the *TRAC* locus with CRISPR/Cas9 enhances tumour rejection. *Nature* **543**, 113–117 (2017).
45. A. P. Rapoport, E. A. Stadtmauer, G. K. Binder-Scholl, O. Goloubeva, D. T. Vogl, S. F. Lacey, A. Z. Badros, A. Garfall, B. Weiss, J. Finklestein, I. Kulikovskaya, S. K. Sinha, S. Kronsberg, M. Gupta, S. Bond, L. Melchiori, J. E. Brewer, A. D. Bennett, A. B. Gerry, N. J. Pumphrey, D. Williams, H. K. Tayton-Martin, L. Ribeiro, T. Holdich, S. Yanovich, N. Hardy, J. Yared, N. Kerr, S. Philip, S. Westphal, D. L. Siegel, B. L. Levine, B. K. Jakobsen, M. Kalos, C. H. June, NY-ESO-1–specific TCR–engineered T cells mediate sustained antigen-specific antitumor effects in myeloma. *Nat. Med.* **21**, 914–921 (2015).
46. Y. Li, R. Moysey, P. E. Molloy, A. L. Vuidepot, T. Mahon, E. Baston, S. Dunn, N. Liddy, J. Jacob, B. K. Jakobsen, J. M. Boulter, Directed evolution of human T-cell receptors with picomolar affinities by phage display. *Nat. Biotech.* **23**, 349–354 (2005).
47. M. Lever, H. S. Lim, P. Kruger, J. Nguyen, N. Trendel, E. Abu-Shah, P. K. Maini, P. A. van der Merwe, O. Dushek, Architecture of a minimal signaling pathway explains the T-cell response to a 1 million-fold variation in antigen affinity and dose. *Proc. Natl. Acad. Sci. U.S.A.* **113**, E6630–E6638 (2016).
48. M. Aleksic, O. Dushek, H. Zhang, E. Shenderov, J. L. Chen, V. Cerundolo, D. Coombs, P. A. van der Merwe, Dependence of T cell antigen recognition on T cell receptor-peptide MHC confinement time. *Immunity* **32**, 163–174 (2010).
49. O. Dushek, M. Aleksic, R. J. Wheeler, H. Zhang, S.-P. Cordoba, Y.-C. Peng, J.-L. Chen, V. Cerundolo, T. Dong, D. Coombs, P. A. van der Merwe, Antigen potency and maximal efficacy reveal a mechanism of efficient T cell activation. *Sci. Signal.* **4**, ra39 (2011).
50. G. Iezzi, K. Karjalainen, A. Lanzavecchia, The duration of antigenic stimulation determines the fate of naive and effector T cells. *Immunity* **8**, 89–95 (1998).
51. D. T. Harris, M. V. Hager, S. N. Smith, Q. Cai, J. D. Stone, P. Kruger, M. Lever, O. Dushek, T. M. Schmitt, P. D. Greenberg, D. M. Kranz, Comparison of T cell activities mediated by human TCRs and CARs that use the same recognition domains. *J. Immunol.* , 1088–1100 (2017).
52. F. Salerno, N. A. Paolini, R. Stark, M. von Lindern, M. C. Wolkers, Distinct PKC-mediated posttranscriptional events set cytokine production kinetics in $CD8^+$ T cells. *Proc. Natl. Acad. Sci. U.S.A.* **114**, 9677–9677 (2017).
53. M. von Essen, C. Menné, B. L. Nielsen, J. P. H. Lauritsen, J. Dietrich, P. S. Andersen, K. Karjalainen, N. Ødum, C. Geisler, The CD3γ leucine-based receptor-sorting motif is required for efficient ligand-mediated TCR down-regulation. *J. Immunol.* **168**, 4519–4523 (2002).
54. C. Utzny, D. Coombs, S. Müller, S. Valitutti, Analysis of peptide/MHC-induced TCR downregulation: Deciphering the triggering kinetics. *Cell Biochem. Biophys.* **46**, 101–112 (2006).
55. S. Thomas, S. A. Xue, C. R. M. Bangham, B. K. Jakobsen, E. C. Morris, H. J. Stauss, Human T cells expressing affinity-matured TCR display accelerated responses but fail to recognize low density of MHC-peptide antigen. *Blood* **118**, 319–329 (2011).
56. J. Sousa, J. Carneiro, A mathematical analysis of TCR serial triggering and down-regulation. *Eur. J. Immunol.* **30**, 3219–3227 (2000).
57. G. Altan-Bonnet, R. N. Germain, Modeling T cell antigen discrimination based on feedback control of digital Erk responses. *PLOS Biol.* **3**, e356 (2005).
58. J. Das, M. Ho, J. Zikherman, C. Govern, M. Yang, A. Weiss, A. K. Chakraborty, J. P. Roose, Digital signaling and hysteresis characterize Ras activation in lymphoid cells. *Cell* **136**, 337–351 (2009).
59. M. N. Navarro, C. Feijoo-Carnero, A. G. Arandilla, M. Trost, D. A. Cantrell, Protein kinase D2 is a digital amplifier of T cell receptor–stimulated diacylglycerol signaling in naive $CD8^+$ T cells. *Sci. Signal* **7**, ra99 (2014).
60. T. Toni, D. Welch, N. Strelkowa, A. Ipsen, M. P. H. Stumpf, Approximate Bayesian computation scheme for parameter inference and model selection in dynamical systems. *J. R. Soc. Interface* **6**, 187–202 (2009).
61. A. Murtaza, V. K. Kuchroo, G. J. Freeman, Changes in the strength of co-stimulation through the B7/CD28 pathway alter functional T cell responses to altered peptide ligands. *Int. Immunol.* **11**, 407–416 (1999).
62. F. Michel, G. Attal-Bonnefoy, G. Mangino, S. Mise-Omata, O. Acuto, CD28 as a molecular amplifier extending TCR ligation and signaling capabilities. *Immunity* **15**, 935–945 (2001).
63. J. A. Siller-Farfán, O. Dushek, Molecular mechanisms of T cell sensitivity to antigen. *Immunol. Rev.* **285**, 194–205 (2018).
64. M. V. Maus, J. Plotkin, G. Jakka, G. Stewart-Jones, I. Rivière, T. Merghoub, J. Wolchok, C. Renner, M. Sadelain, An MHC-restricted antibody-based chimeric antigen receptor requires TCR-like affinity to maintain antigen specificity. *Mol. Ther. Oncolytics* **3**, 1–1 (2016).
65. G. Stewart-Jones, A. Wadle, A. Hombach, E. Shenderov, G. Held, E. Fischer, S. Kleber, N. Nuber, F. Stenner-Liewen, S. Bauer, A. McMichael, A. Knuth, H. Abken, A. A. Hombach, V. Cerundolo, E. Y. Jones, C. Renner, Rational development of high-affinity T-cell receptor-like antibodies. *Proc. Natl. Acad. Sci. U.S.A.* **106**, 5784–5788 (2009).
66. Q. Han, N. Bagheri, E. M. Bradshaw, D. A. Hafler, D. A. Lauffenburger, J. C. Love, Polyfunctional responses by human T cells result from sequential release of cytokines. *Proc. Natl. Acad. Sci. U.S.A.* **109**, 1607–1612 (2012).
67. F. Macián, F. Garćia-Cózar, S. H. Im, H. F. Horton, M. C. Byrne, A. Rao, Transcriptional mechanisms underlying lymphocyte tolerance. *Cell* **109**, 719–731 (2002).
68. A. D. Wells, New insights into the molecular basis of T cell anergy: Anergy factors, avoidance sensors, and epigenetic imprinting. *J. Immunol.* **182**, 7331–7341 (2009).
69. F. Marangoni, T. T. Murooka, T. Manzo, E. Y. Kim, E. Carrizosa, N. M. Elpek, T. R. Mempel, The transcription factor NFAT exhibits signal memory during serial T cell interactions with antigen-presenting cells. *Immunity* **38**, 237–249 (2013).
70. O. Acuto, F. Michel, CD28-mediated co-stimulation: A quantitative support for TCR signaling. *Nat. Rev. Immunol.* **3**, 939–951 (2003).
71. L. Chen, D. B. Flies, Molecular mechanisms of T cell co-stimulation and co-inhibition. *Nat. Rev. Immunol.* **13**, 227–242 (2013).
72. T. Pradeu, E. Vivier, The discontinuity theory of immunity. *Sci. Immunol.* **1**, AAG0479 (2016).
73. K. Smith, B. Seddon, M. A. Purbhoo, R. Zamoyska, A. G. Fisher, M. Merkenschlager, Sensory adaptation in naive peripheral CD4 T cells. *J. Exp. Med.* **194**, 1253–1262 (2001).
74. L. Chiodetti, S. Choi, D. L. Barber, R. H. Schwartz, Adaptive tolerance and clonal anergy are distinct biochemical states. *J. Immunol.* **176**, 2279–2291 (2006).
75. R. M. Teague, P. D. Greenberg, C. Fowler, M. Z. Huang, X. Tan, J. Morimoto, M. L. Dossett, E. S. Huseby, C. Öhlén, Peripheral $CD8^+$ T cell tolerance to self-proteins is regulated proximally at the T cell receptor. *Immunity* **28**, 662–674 (2008).
76. T. Honda, J. G. Egen, T. Lämmermann, W. Kastenmüller, P. Torabi-Parizi, R. N. Germain, Tuning of antigen sensitivity by T cell receptor-dependent negative feedback controls T cell effector function in inflamed tissues. *Immunity* **40**, 235–247 (2014).
77. A. O. Kamphorst, A. Wieland, T. Nasti, S. Yang, R. Zhang, D. L. Barber, B. T. Konieczny, C. Z. Daugherty, L. Koenig, K. Yu, G. L. Sica, A. H. Sharpe, G. J. Freeman, B. R. Blazar, L. A. Turka, T. K. Owonikoko, R. N. Pillai, S. S. Ramalingam, K. Araki, R. Ahmed, Rescue of exhausted CD8 T cells by PD-1–targeted therapies is CD28-dependent. *Science* **355**, 1423–1427 (2017).
78. B. Savoldo, C. A. Ramos, E. Liu, M. P. Mims, M. J. Keating, G. Carrum, R. T. Kamble, C. M. Bollard, A. P. Gee, Z. Mei, H. Liu, B. Grilley, C. M. Rooney, H. E. Heslop, M. K. Brenner,

G. Dotti, Cd28 costimulation improves expansion and persistence of chimeric antigen receptor-modified T cells in lymphoma patients. *J. Clin. Invest.* **121**, 1822–1826 (2011).
79. R. J. Brentjens, E. Santos, Y. Nikhamin, R. Yeh, M. Matsushita, K. la Perle, A. Quintás-Cardama, S. M. Larson, M. Sadelain, Genetically targeted T cells eradicate systemic acute lymphoblastic leukemia xenografts. *Clin. Cancer Res.* **13**, 5426–5435 (2007).
80. C. Carpenito, M. C. Milone, R. Hassan, J. C. Simonet, M. Lakhal, M. M. Suhoski, A. Varela-Rohena, K. M. Haines, D. F. Heitjan, S. M. Albelda, R. G. Carroll, J. L. Riley, I. Pastan, C. H. June, Control of large, established tumor xenografts with genetically retargeted human T cells containing Cd28 and Cd137 domains. *Proc. Natl. Acad. Sci. U.S.A.* **106**, 3360–3365 (2009).
81. Z. Zhao, M. Condomines, S. J. C. van der Stegen, F. Perna, C. C. Kloss, G. Gunset, J. Plotkin, M. Sadelain, Structural design of engineered costimulation determines tumor rejection kinetics and persistence of CAR T cells. *Cancer Cell* **28**, 415–428 (2015).
82. M. A. Pulè, K. C. Straathof, G. Dotti, H. E. Heslop, C. M. Rooney, M. K. Brenner, A chimeric T cell antigen receptor that augments cytokine release and supports clonal expansion of primary human T cells. *Mol. Ther.* **12**, 933–941 (2005).
83. A. Wyzgol, N. Müller, A. Fick, S. Munkel, G. U. Grigoleit, K. Pfizenmaier, H. Wajant, Trimer stabilization, oligomerization, and antibody-mediated cell surface immobilization improve the activity of soluble trimers of CD27L, CD40L, 41BBL, and glucocorticoid-induced TNF receptor ligand. *J. Immunol.* **183**, 1851–1861 (2009).
84. J. L. L. Chen, P. R. Dunbar, U. Gileadi, E. Jäger, S. Gnjatic, Y. Nagata, E. Stockert, D. L. Panicali, Y. T. Chen, A. Knuth, L. J. Old, V. Cerundolo, Identification of NY-ESO-1 peptide analogues capable of improved stimulation of tumor-reactive CTL. *J. Immunol.* **165**, 948–955 (2000).
85. G. Jakka, P. C. Schuberth, M. Thiel, G. Held, F. Stenner, M. van den Broek, C. Renner, A. Mischo, U. Petrausch, Antigen-specific in vitro expansion of functional redirected Ny-Eso-1-specific human $CD8^+$ T-cells in a cell-free system. *Anticancer Res* **33**, 4189–4201 (2013).
86. M. P. Tan, A. B. Gerry, J. E. Brewer, L. Melchiori, J. S. Bridgeman, A. D. Bennett, N. J. Pumphrey, B. K. Jakobsen, D. A. Price, K. Ladell, A. K. Sewell, T cell receptor binding affinity governs the functional profile of cancer-specific $CD8^+$ T cells. *Clin. Exp. Immunol.* **180**, 255–270 (2015).

Acknowledgments: We thank S. J. Davis for providing the CD86 expression plasmids, H. Wajant for providing the 4-1BBL expression plasmids, C. Renner for providing the T1 CAR plasmids, A. Rendall and V. Shahrezaei for the feedback on mathematical modeling, Adaptimmune Ltd. for providing the c58c61 TCR, and E. Abu Shah, M. L. Dustin, M. H. Brown, and V. Cerundolo for the helpful discussions about experimental protocols. We thank P. A. van der Merwe for a critical reading of the manuscript. **Funding:** This work was supported by a Doctoral Training Centre Systems Biology studentship from the Engineering and Physical Sciences Research Council (to N.T.), a scholarship from the Konrad Adenauer Stiftung (to N.T.), a studentship from the Edward Penley Abraham Trust and Exeter College, Oxford (to P.K.), a Wellcome Trust PhD Studentship in Science (203737/Z/16/Z, to J.P.), a postdoctoral extension award from the Cellular Immunology Unit Trust (to P.K.), a Sir Henry Dale Fellowship jointly funded by the Wellcome Trust and the Royal Society (098363, to O.D.), pump-prime funding from the Cancer Research UK Oxford Centre Development Fund (CRUKDF 0715, to O.D.), NSF (USA) grant (1817936, to E.D.S.), and a Wellcome Trust Senior Research Fellowship (207537/Z/17/Z, to O.D.). **Author contributions:** N.T., P.K., S.G., J.N., and J.P. performed the experiments; N.T., P.K., E.D.S., and O.D. performed the mathematical modeling; N.T., P.K., S.G., J.N., J.P., and O.D. analyzed the data; N.T., P.K., and O.D. designed the research and wrote the paper; and all authors discussed the results and commented on the paper. **Competing interests:** The authors declare that they have no competing interests. **Data and materials availability:** All data needed to evaluate the conclusions in the paper are present in the paper or the Supplementary Materials.

Submitted 30 July 2019
Resubmitted 2 March 2020
Accepted 23 December 2020
Published 19 January 2021
10.1126/scisignal.aay9363

Citation: N. Trendel, P. Kruger, S. Gaglione, J. Nguyen, J. Pettmann, E. D. Sontag, O. Dushek, Perfect adaptation of $CD8^+$ T cell responses to constant antigen input over a wide range of affinities is overcome by costimulation. *Sci. Signal.* **14**, eaay9363 (2021).

Science Signaling

Perfect adaptation of CD8$^+$ T cell responses to constant antigen input over a wide range of affinities is overcome by costimulation

Nicola Trendel, Philipp Kruger, Stephanie Gaglione, John Nguyen, Johannes Pettmann, Eduardo D. Sontag and Omer Dushek

Sci. Signal. **14** (666), eaay9363.
DOI: 10.1126/scisignal.aay9363

Adapting to antigens

Cell surface T cell receptors (TCRs) are engaged by antigens, leading to T cell activation and cytokine production. Trendel *et al*. exposed primary human CD8$^+$ T cells to a wide range of antigens and mathematically analyzed cellular cytokine production to determine both how T cells respond to constant antigen stimulation and the effect of down-regulation of the TCR from the cell surface. The authors showed that T cells adapted to constant antigen stimulation by stopping cytokine production even in the absence of complete TCR down-regulation. Signaling by costimulatory receptors broke this adaptation and maintained cytokine production. These results have implications for the design of chimeric antigen receptors that must maintain cellular activation to provide effective therapies.

Science Signaling
AAAS

stke.sciencemag.org/cgi/content/full/14/666/eaay9363/DC1

Supplementary Materials for

Perfect adaptation of CD8$^+$ T cell responses to constant antigen input over a wide range of affinities is overcome by costimulation

Nicola Trendel, Philipp Kruger, Stephanie Gaglione, John Nguyen, Johannes Pettmann, Eduardo D. Sontag, Omer Dushek*

*Corresponding author. Email: omer.dushek@path.ox.ac.uk

Published 19 January 2021, *Sci. Signal.* **14**, eaay9363 (2021)
DOI: 10.1126/scisignal.aay9363

This PDF file includes:

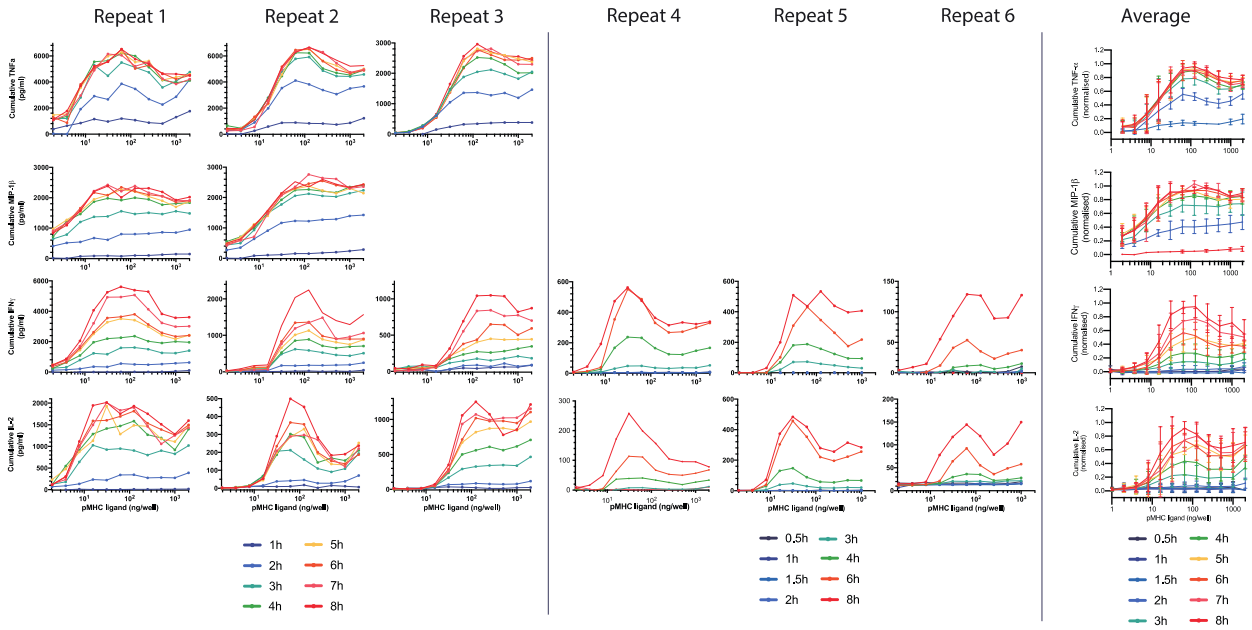

Fig. S1. Cytokine production by T cells in response to constant stimulation by the supraphysiological affinity pMHC 9V. Expanded data from Fig. 2B showing the cumulative amounts of TNF-α, MIP-1β, IFN-γ, and IL-2 for individual repeats (six left columns) together with the averaged data (right). The averaged TNF-α data are the same as those shown in Fig. 2B. Error bars represent the SD.

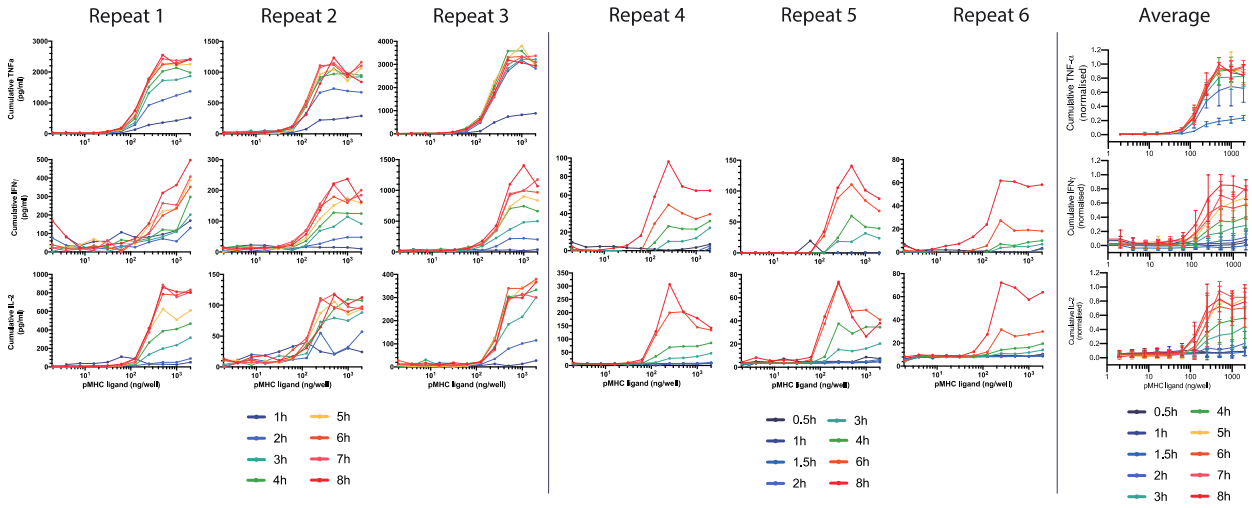

Fig. S2. Cytokine production by T cells in response to constant stimulation by the physiological affinity pMHC 4A8K. Expanded data from Fig. 2B showing the cumulative amounts of TNF-α, IFN-γ, and IL-2 for individual repeats (six left columns) together with the averaged data (right). The averaged TNF-α data are the same as those shown in Fig. 2B. Error bars represent the SD.

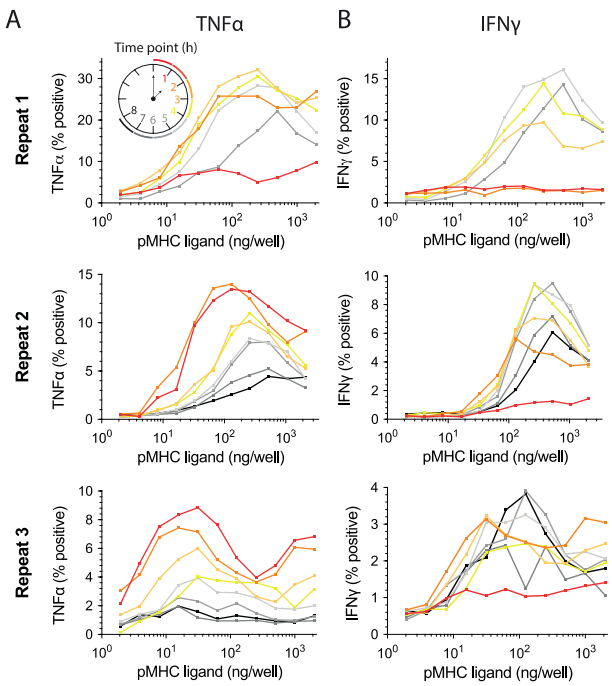

Fig. S3. T cell adaptation is the result of reduced cytokine production per cell. (**A** and **B**) T cells were stimulated with the indicated concentrations of 9V pMHC for the indicated times (1 to 8 hours) before being subjected to intracellular cytokine staining of (A) TNF-α and (B) IFN-γ by flow cytometry. Cytokine secretion was blocked by the addition of Brefeldin A for the last hour of the stimulation. Data are shown for three independent repeats.

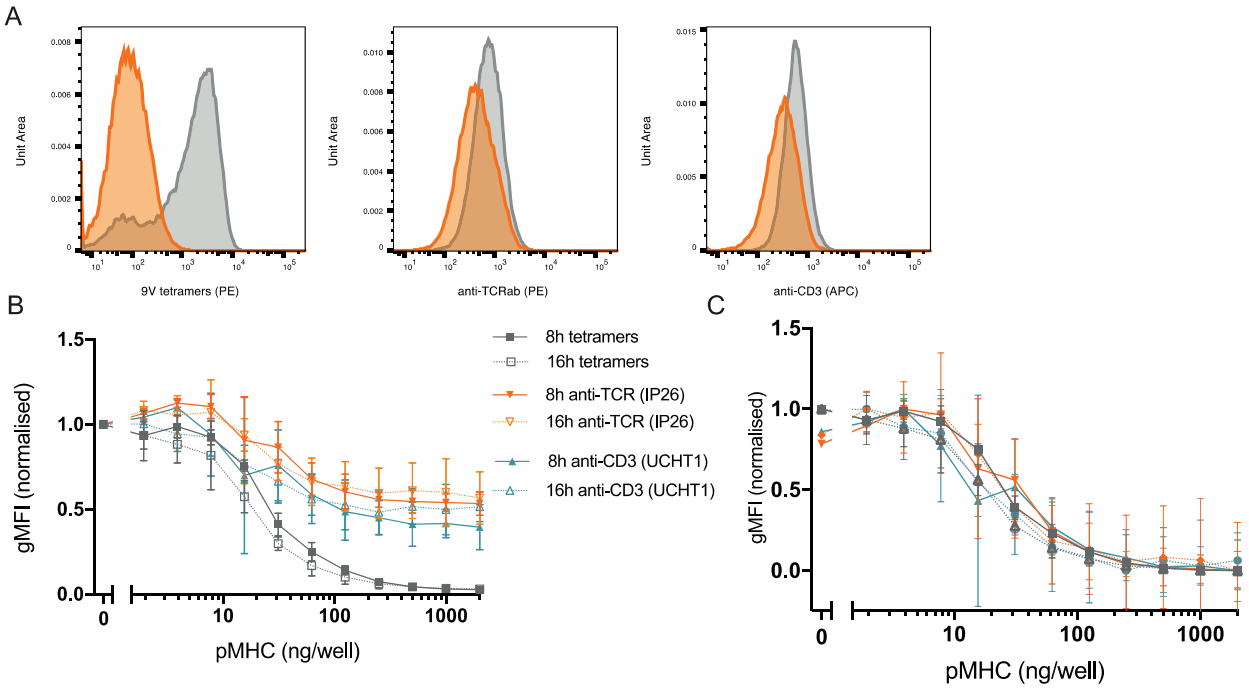

Fig. S4. Quantitative assessment of TCR down-regulation is independent of the detection method used. (**A**) Flow cytometry histograms comparing TCR expression on unstimulated (gray) and pMHC-stimulated (orange) T cells using pMHC tetramers (left), anti-TCRαβ antibody clone IP26 (center), and anti-CD3ε antibody clone UCHT1 (right). The different expression pattern is a result of only a subset of T cells expressing the c58c61 TCR, which is seen by the bimodal distribution in pMHC tetramer stain. (**B**) Geometric mean fluorescence intensity (gMFI) over the concentration of pMHC for the indicated detection reagent normalized to the gMFI of unstimulated T cells ([pMHC] = 0 ng/well). The fold-reduction is smaller when using antibodies for detection because they detect all surface TCR (both the pMHC-specific c58c61 TCR that is downregulated and any nonspecific TCRs that are not downregulated). (**C**) Renormalizing the data from the experiments in (B) to span 0 to 1 shows that all detection methods were quantitatively similar.

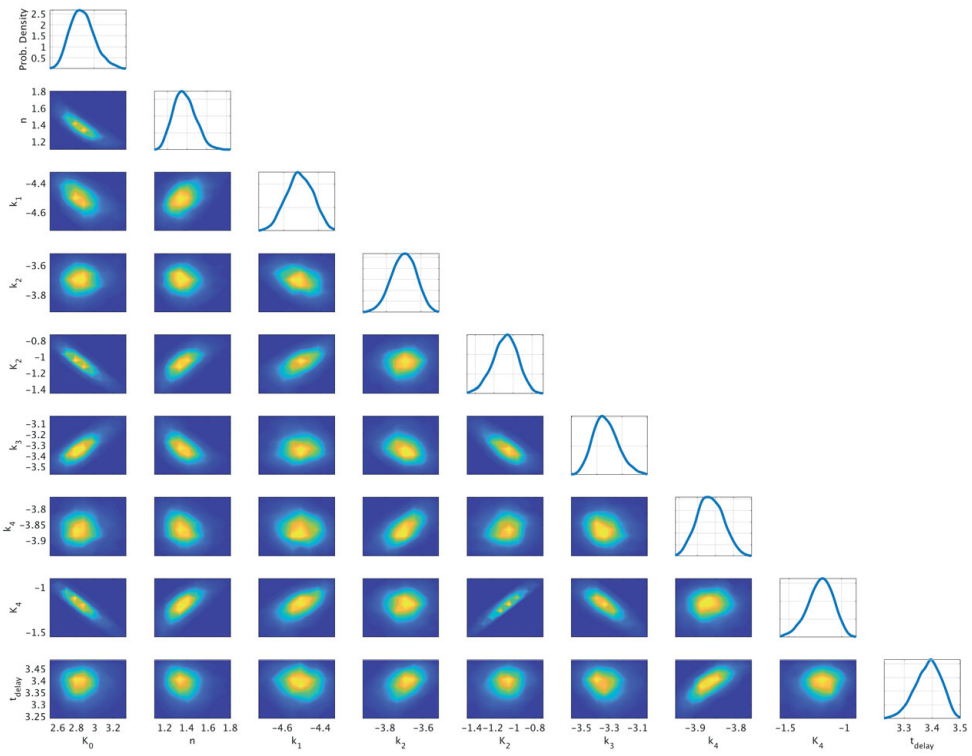

Fig. S5. Posterior distributions of 3000 particles after 30 populations using ABC-SMC. The marginal distribution of each parameter is shown on the diagonal with off-diagonal heatmaps displaying pair correlations. See Materials and Methods for further details.

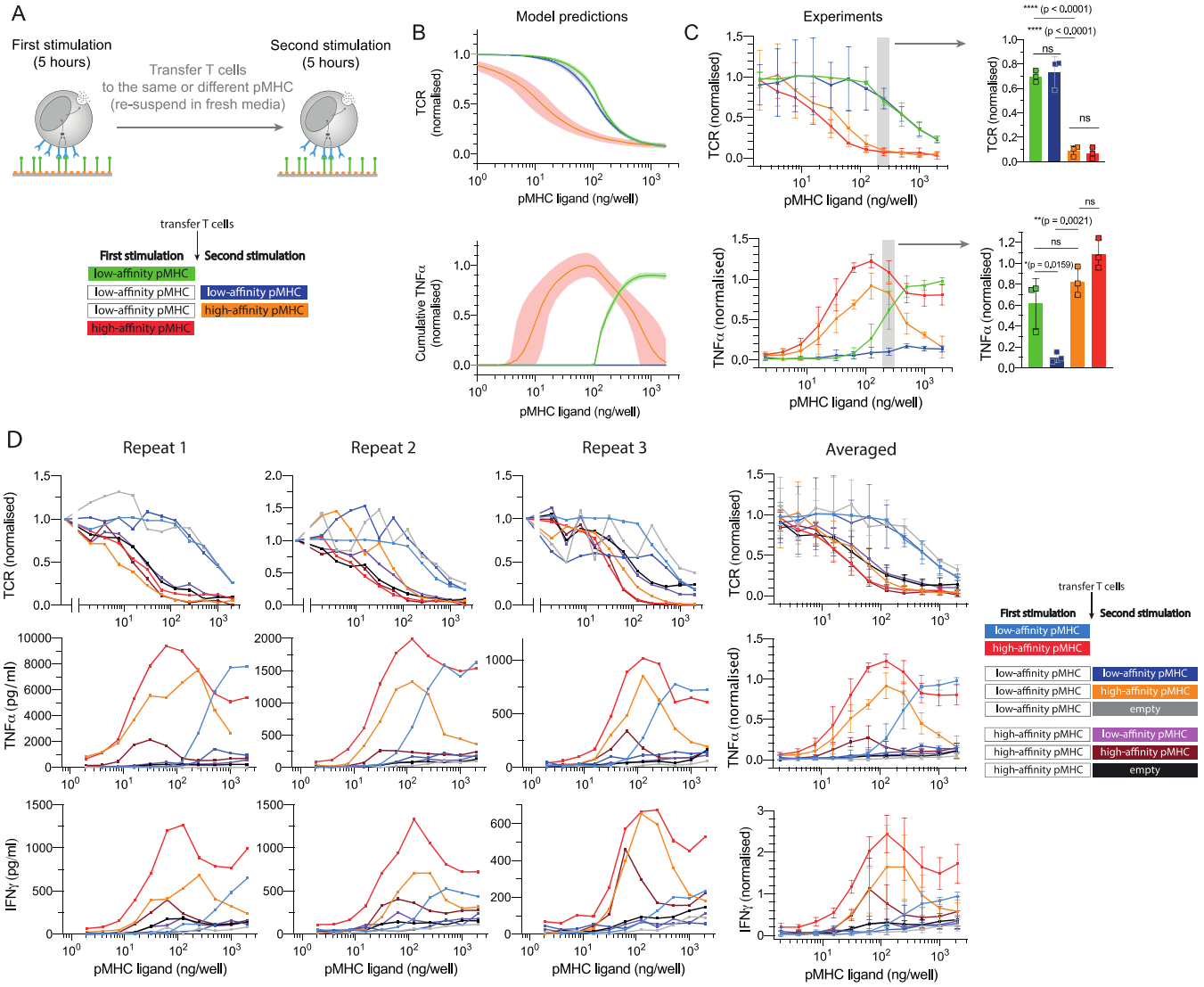

Fig. S6. T cells adapted to a low-affinity antigen can be reactivated with a higher-affinity antigen. (**A**) Schematic of the experiment showing that T cells were first stimulated for 5 hours on the low-affinity antigen before being transferred for a second stimulation of 5 hours with the same or different pMHC antigen (at the same antigen concentration). (**B**) Predicted TCR surface expression (top) and cytokine production (bottom) for the transfer experiment by the mathematical model. (**C**) TCR surface expression (top) and TNF-α production (bottom) with a detailed comparison performed at the indicated concentration (right). Consistent with the adaptation phenotype, a first stimulation with the low-affinity pMHC 4A8K (green) led to reduced cytokine production in a second stimulation on the same pMHC (blue). However, transferring T cells to the higher-affinity pMHC 9V led to further TCR downregulation and further cytokine production (orange). Note that beyond the gray shaded region, cytokine production is progressively reduced, which the model predicts is a result of lower levels of surface TCR before transfer to the higher affinity pMHC. Data are means and SD of three independent experiments with statistical significance determined by ordinary one-way ANOVA corrected for multiple comparisons by Dunnett's test. (**D**) Individual repeats (left three columns) and averaged data (right) showing TCR, TNF-α, and IFN-γ for all transfer conditions (see legend on right), including transfers from the high-affinity (9V) to the low-affinity (4A8K) pMHC, showing that decreasing antigen affinity does not induce cytokine production (light purple). The averaged data in (C) is taken from the averaged data in (D) and shows a subset of all the conditions tested.

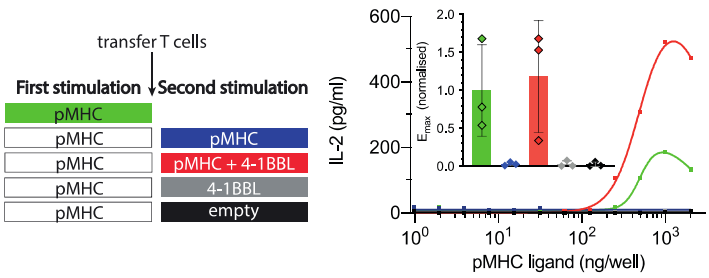

Fig. S7. T cells adapted to constant antigen can be reactivated with 4-1BB costimulation. Expanded data showing IL-2 secretion for the experiment shown in Fig. 4D.

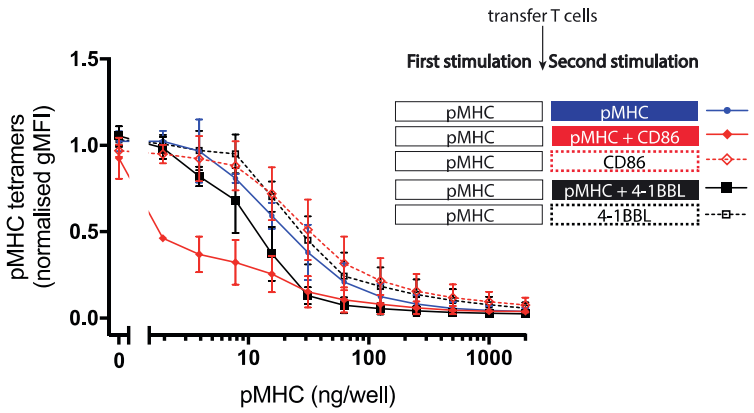

Fig. S8. Costimulation by CD28 and 4-1BB does not increase TCR surface expression after adaptation. Expanded data showing TCR surface expression from the T cell transfer experiments shown in Fig. 4.

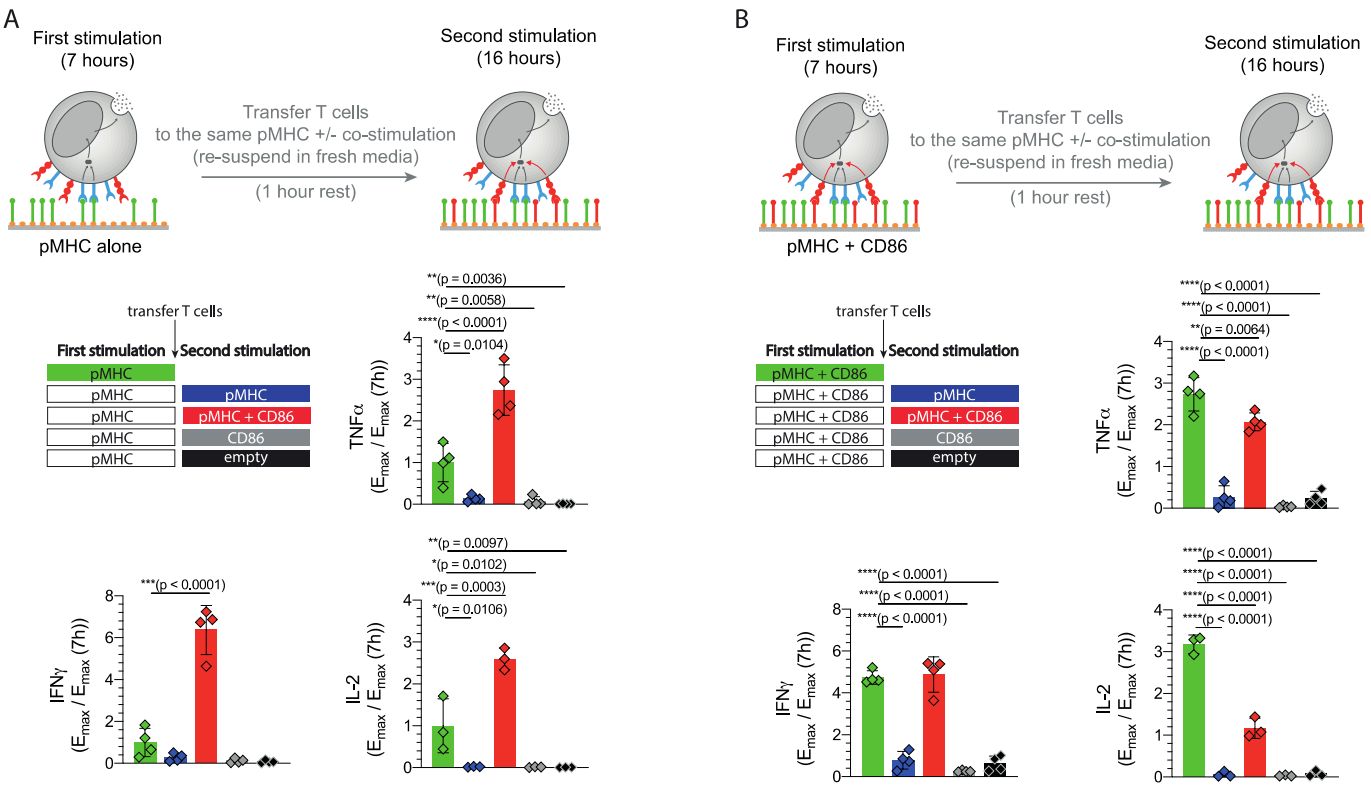

Fig. S9. CD28 costimulation does not prevent adaptation to constant antigen stimulation. (**A** and **B**) Primary human CD8$^+$ effector T cells expressing the c58c61 TCR were stimulated with a range of concentrations of the low-affinity pMHC antigen 4A8K and the concentrations of TNF-α, IFN-γ, and IL-2 in the culture medium were measured by ELISA. T cells were first stimulated for 7 hours with the low-affinity pMHC 4A8K with or without recombinant CD86 (light blue lines). The T cells were rested for 1 hour in fresh medium before being transferred into fresh medium to pMHC alone (dark blue), pMHC and CD86 (red), CD86 alone (gray), or to empty wells (black). (A) Schematic of the transfer experiment with pMHC alone in the first stimulation (top) together with the averaged E_{max} values from four independent experiments for TNF-α, IFN-γ, and IL-2 (bottom). B) Schematic of transfer experiment with pMHC and CD86 in the first stimulation (top) along with averaged E_{max} values from four independent experiments for TNF-α, IFN-γ, and IL-2 (bottom). All data were normalized to the value of E_{max} at 7 hours with pMHC alone. Error bars represent the SD, and statistical significance was determined by ordinary one-way ANOVA corrected for multiple comparisons by Dunnett's test comparing all conditions to the value of E_{max} during the first stimulation.

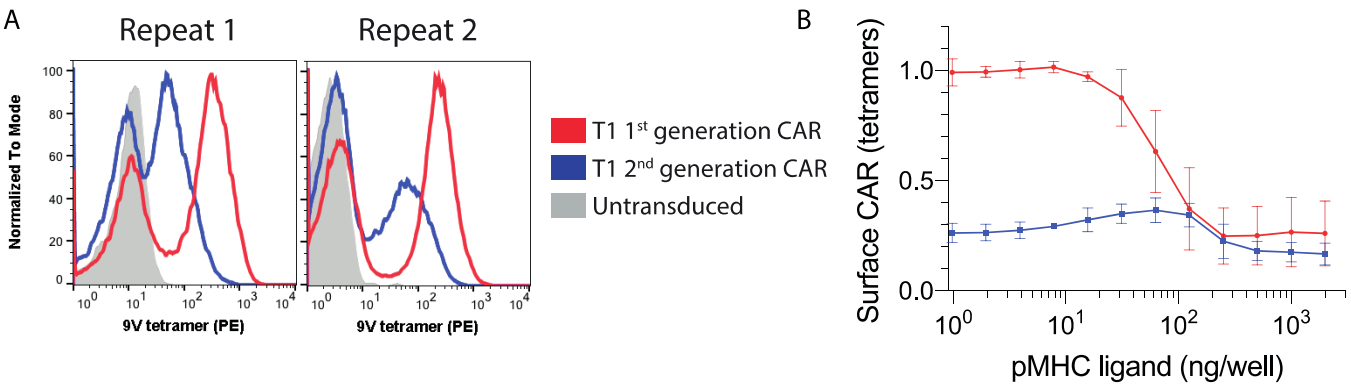

Fig. S10. Expression levels and antigen-induced down-regulation of first- and second-generation CARs. (**A**) T cells expressing the first- and second-generation T1 CAR were stained with 9V pMHC tetramers and CAR expression was measured by flow cytometry. (**B**) CAR-T cells were stimulated with the indicated titration of the 9V pMHC antigen for 8 hours and then surface CAR expression was measured with pMHC tetramers. Data are the average of at least three independent experiments and error bars represent SD.